Geol. Mag. **144** (*6*), *2007, pp. 987–1013. © 2007 Cambridge University Press*
doi:10.1017/S0016756807003780 First published online 21 August 2007 *Printed in the United Kingdom*

Last Interglacial (Eemian) hydrographic conditions in the southwestern Baltic Sea based on dinoflagellate cysts from Ristinge Klint, Denmark

MARTIN J. HEAD*

Department of Earth Sciences, Brock University, 500 Glenridge Avenue, St. Catharines, Ontario L2S 3A1, Canada

(*Received* 23 August 2006; *accepted* 18 January 2007)

Abstract – A dinoflagellate cyst record with strong Mediterranean/Lusitanian affinities is described from marine deposits of Eemian age (Last Interglacial; Late Pleistocene) at Ristinge Klint, Denmark, revealing new information about the hydrographic evolution of the southwestern Baltic Sea. A revised correlation of the pollen record at Ristinge Klint with that of the annually laminated site at Bispingen in northern Germany provides temporal control. Approximately the first quarter of Eemian time is represented. A marine ingression into a lake took place during the *Quercus* rise, about 300 years into the interglacial, and is marked by low (< *c*. 3 psu) salinities at the base of the Cyprina Clay that increased progressively. An abrupt and significant rise in the inflow of warm, saline waters from the North Sea occurred at about 750 years into the interglacial (the *Corylus* rise), and at about 1900 years into the interglacial, strongly stratified waters developed. Higher in the Cyprina Clay and continuing to its top, at nearly 3000 years into the interglacial, more open-marine waters are indicated, although fully marine conditions were not reached. The dinoflagellate record throughout the Cyprina Clay at Ristinge Klint is therefore one of increasing marine influence. Summer sea-surface temperatures approached, and may have exceeded, 26–28 °C during early Eemian time, indicating temperatures at least 5 °C warmer than at present. These warm conditions persisted to the top of the record at Ristinge Klint. No evidence exists at Ristinge Klint for the influence of Arctic watermasses, and the paucity of cold-water species throughout the section reflects mild winter temperatures in the southwestern Baltic Sea.
The new species *Spiniferites ristingensis* is formally described, and the name *Operculodinium centrocarpum* var. *cezare* de Vernal, Goyette & Rodrigues, 1989 is validated.

Keywords: dinoflagellate cysts, Eemian, Last Interglacial, Quaternary, Baltic Sea.

1. Introduction

The Last Interglacial (Eemian Stage) is approximately equivalent to Marine Isotope Substage (MIS) 5e (Sánchez Goñi *et al*. 1999, 2000). The Eemian probably lasted for no more than 13 000 years in northern Europe (Turner, 2002), although uncertainty in the relationship between its onset and that of MIS 5e has led to disagreement over the precise timing of the start of the Eemian, with dates of about 126 ka (Shackleton *et al*. 2003) and 131 ka (Beets, Beets & Cleveringa, 2006) being proposed. In any case, sea levels had reached modern levels by 129 ± 1 ka (Overpeck *et al*. 2006), and Northern Hemisphere summer insolation peaked between 131 and 127 ka (Cape Last Interglacial Project Members, 2006). The Eemian is the most accessible interglacial after the present, and Eemian climates were generally warmer than today (CLIMAP, 1984; Sejrup & Larsen, 1991). This is especially true of the Arctic, where summers may have averaged 5 °C warmer than present (Cape Last Interglacial Project Members, 2006). The Eemian therefore provides a potential analogue for future global warming. Global sea level was probably a few metres higher than at present (Shackleton *et al*. 2003; Otto-Bliesner *et al*. 2006), but relative sea level in the Baltic region was affected also by glacioisostatic depression and subsequent rebound.

The cliff section at Ristinge Klint (54.51° N, 10.38° E; Fig. 1) on Langeland, southern Denmark, has long been known to contain interglacial deposits of Eemian age (e.g. Madsen, Nordmann & Hartz, 1908; Sjørring *et al.* 1982). Their age has been reaffirmed by modern pollen analysis (Kristensen *et al*. 2000) and amino acid studies (Sejrup & Knudsen, 1999). These Eemian deposits are about 3 m thick and consist of freshwater clay and sand overlain by marine clay. They, in turn, are overlain by Weichselian glaciofluvial deposits and tills, and the entire succession has been pushed into repeating thrust slices by late Weichselian ice advances (Kristensen *et al*. 2000). Recent studies of the pollen, benthic foraminifers and ostracodes at Ristinge Klint (Kristensen *et al*. 2000) have provided a detailed palaeoenvironmental and vegetational history of this site during the early Eemian. Pollen chronology shows that the sequence represents almost 3000 years, that is, about the first quarter of Eemian time. Evidence from benthic foraminifers and ostracodes reveals a

*E-mail: mjhead@brocku.ca

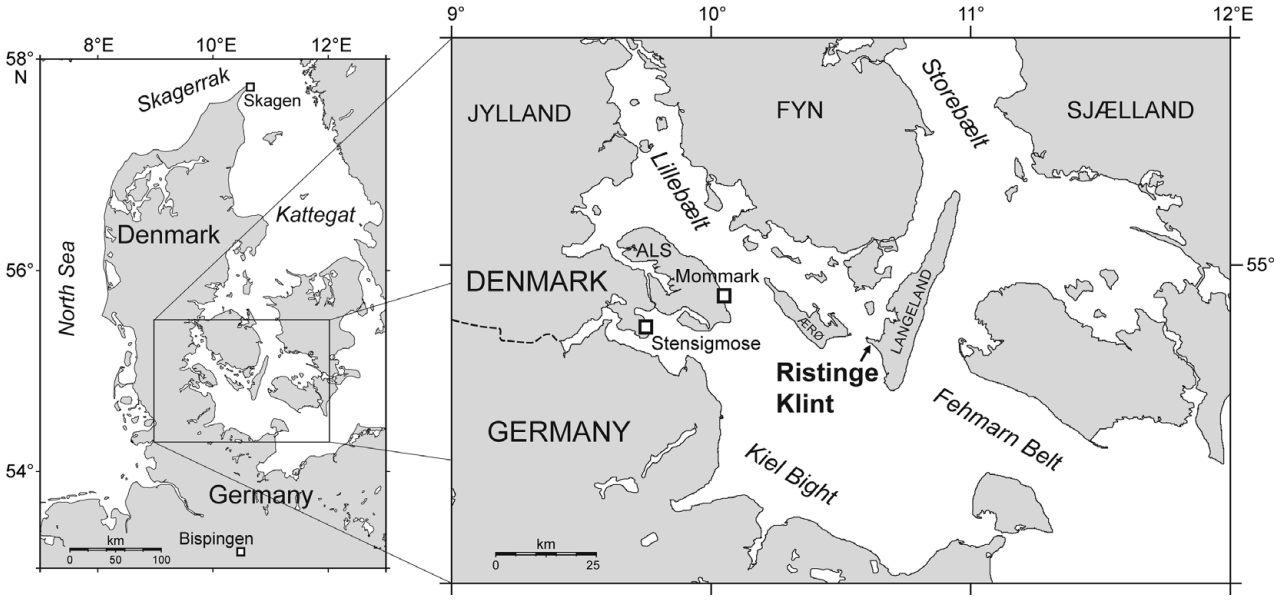

Figure 1. Location map of the western Baltic showing the important marine Eemian sites of Ristinge Klint (this study), Mommark and Stensigmose.

change from freshwater to marine conditions about 300 years into the interglacial, a marked increase in salinity at about 750 years, and a major alteration in current activity at about 1900 years (Kristensen *et al*. 2000, using the chronology adopted herein).

These events and their timing are important for understanding the early Eemian development of the Baltic Sea basin (Fig. 2). This was a time of climatic recovery following the Saalian ice retreat, of terrestrial vegetational change, of residual isostatic depression, and of eustatic rise. A consequence was the opening in the early Eemian of two important seaways into the Baltic Sea. One was located across the Karelian Isthmus connecting the Baltic Sea with the White Sea and Arctic Ocean to the east (Zans, 1936; Raukas, 1991; Donner, 1995) and is thought to have been open for about 2–2.5 ka in the early Eemian (Funder, Demidov & Yelovicheva, 2002). The other occurred in the region of the Belt Sea, remained open throughout the Eemian, and was possibly located along the northern part of Sjælland and southern Sweden rather than the present-day Danish straits of Lillebælt, Storebælt and Øresund (Funder, Demidov & Yelovicheva, 2002). In addition, a narrow connection to the North Sea may have existed across the southern part of the Jutland peninsula in the vicinity of the Kiel Canal (Kosack & Lange, 1985; Knudsen, 1985; Funder, Demidov & Yelovicheva, 2002). This connects to the western Belt Sea where Ristinge Klint is presently located (Fig. 2). Ristinge Klint is therefore well situated for assessing the nature and influence of North Sea water entering the Baltic during the early Eemian.

A useful comparison to Ristinge Klint are ice-pushed Eemian deposits at Mommark, on the island of Als, located only about 40 km to the WNW of Ristinge Klint (Fig. 1). The Mommark deposits, like those at Ristinge Klint, contain the Cyprina Clay and have been studied for pollen (Gibbard & Glaister, 2006), foraminifera and ostracodes (Kristensen & Knudsen, 2006), molluscs (Funder & Balic-Zunic, 2006) and diatoms (Haila, Miettinen & Eronen, 2006). Unlike Ristinge Klint, the Mommark locality has yielded a complete record of Eemian deposition. Analysis of the dinoflagellate cysts at Mommark by the present author is in progress.

The present study is the first to document fully the marine organic-walled dinoflagellate cysts from the Eemian of the southwestern Baltic Sea basin, although the presence of dinoflagellate cysts at Ristinge Klint was noted by Kristensen *et al*. (2000). With the exception of a brief taxonomic investigation (Head, 2003), the only previous detailed studies of Eemian dinoflagellate cysts from the Baltic are from Mertuanoja on the eastern margin of the Gulf of Bothnia (Eriksson, Grönlund & Uutela, 1999) and from a borehole at Licze in northern Poland (Head *et al*. 2005). Both studies indicate much warmer and more saline conditions than at present.

Dinoflagellates live mostly within or near surface waters, and their resting cysts essentially reflect this environment. The present study aims to: (1) elucidate the hydrographic development throughout the marine sequence at Ristinge Klint in terms of summer sea-surface temperature and salinity, and thereby assess the source of watermasses influencing the region; (2) explore hydrographic gradients within the Baltic Sea during the Eemian by comparing with assemblages reported elsewhere; and (3) characterize Eemian dinoflagellate cysts in the southwestern Baltic as a potential means to distinguish Eemian from earlier interglacial deposits in the region. Previous published

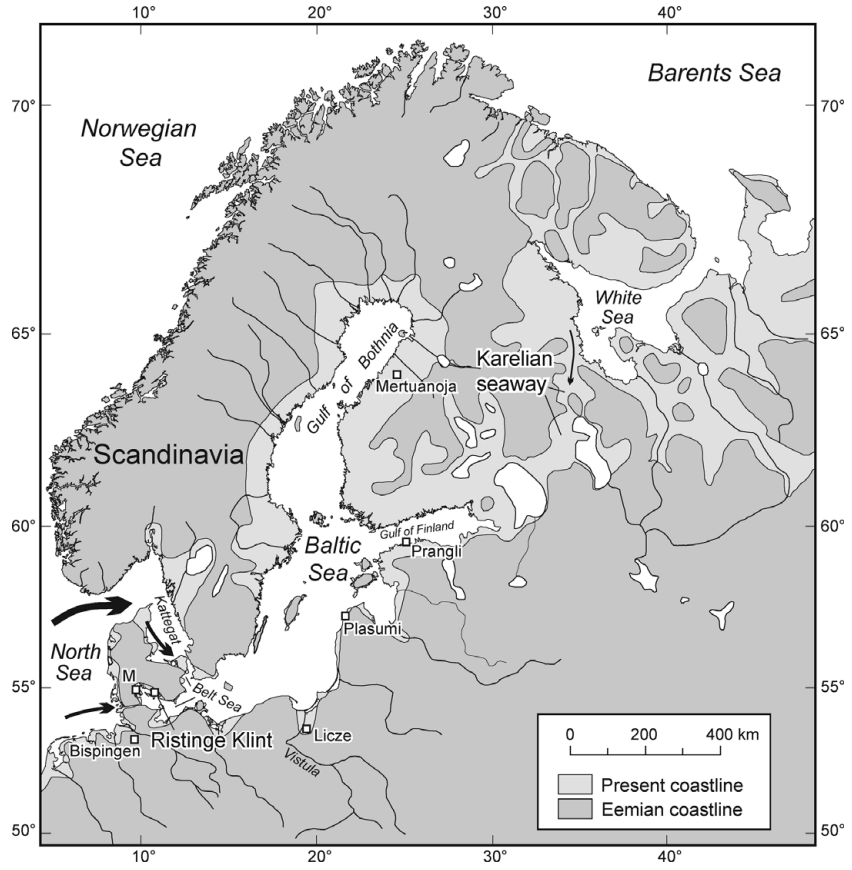

Figure 2. Hydrography and geography of the Baltic Sea region today and during maximum inundation in the early Eemian (based on Funder, Demidov & Yelovicheva, 2002; Head *et al*. 2005). Ristinge Klint is marked, along with other Eemian sites mentioned in the text. M = Mommark.

studies of marine fossils from Ristinge Klint have dealt only with benthic organisms, represented by ostracodes, foraminifera and molluscs (Kristensen *et al*. 2000; Funder, Demidov & Yelovicheva, 2002). The present study allows Eemian surface-water and bottom-water palaeoenvironments to be integrated for the first time at Ristinge Klint.

2. Present hydrography of the southwestern Baltic Sea

The Baltic Sea presently receives saline water only from the North Sea, which enters through the Danish Belts as bottom water, with brackish water from the Baltic Sea flowing out through the Danish Belts as surface waters. The shallow sill depth of the Danish Belts restricts the inflow of saline water, so that freshwater runoff and precipitation into the Baltic Sea exceeds the inflow of saline water. This results in increasingly brackish conditions from west to east across the Baltic Sea. In the Kiel Bight, southwestern Baltic, August sea-surface temperatures are typically about 17–22 °C, and salinities are 12–18 at 8 m depth (Bundesamt für Seeschifffahrt und Hydrographie, unpub. data, 2006: http://www.bsh.de/en/Marine %20data/Observations/Climate/index.jsp). Winter sea-surface temperatures typically do not exceed 4 °C in the Kiel Bight. Waters in the Kiel Bight, as elsewhere in the Baltic, are moderately stratified.

3. Distribution of dinoflagellates in the modern Baltic Sea

The distribution of modern dinoflagellate cysts in bottom sediments of the Baltic Sea has not been documented consistently. Cysts are known principally from the following areas: outer Skagerrak (Rochon *et al*. 1999), Oslofjord (Dale, 1983; Grøsfjeld & Harland, 2001), west coast of Sweden (Persson, Godhe & Karlson, 2000), Kattegat (Ellegaard, Christensen & Moestrup, 1994), the Kiel Bight (Nehring, 1994, 1997) and southern Baltic Sea (Matthiessen & Brenner, 1996), as well as areas off Finland and a long transect between the Kattegat and inner Baltic Sea proper (N. Gundersen, unpub. Cand. Scient. Dissertation, Univ. Oslo, 1988; Dale, 1996). Kiel Bight (Fig. 1) is adjacent to Ristinge Klint and so affords a direct comparison between modern and Eemian conditions in this area.

The distribution of dinoflagellate motile stages in the plankton is relatively well known for the modern Baltic. For example, 178 dinoflagellate species have been reported in the Skagerrak–Kattegat plankton by the

Department of Marine Botany, Göteborg University, Sweden (unpub. data, 2006; checklist of phytoplankton in the Skagerrak–Kattegat (including heterotrophic protists): http://www.marbot.gu.se/sss/ssshome.htm). This report includes and updates those of Throndsen (1969), Heimdal, Hasle & Throndsen (1973), Christensen, Koch & Thomsen (1985) and Hansen & Larsen (1992). For the Baltic Sea proper, the Finnish Institute of Marine Research, Helsinki (unpub. data, 2006; Baltic Sea Alg@line: http://www.fimr.fi/en/itamerikanta/bsds/1731.html) has compiled an extensive biota list, and for the Kiel Bight, plankton records are given in Pankow (1990) and Nehring (1994). A general overview of Baltic Sea phytoplankton distributions is given in Edler, Hälfors & Niemi (1984). Because the corresponding motile stage has been identified for most cyst types (see Head, 1996*a*, for compilation), it is now possible to use these motile-stage plankton records to refine our assessment of the distribution of cyst-producing dinoflagellates in the Baltic Sea today.

4. Eemian succession at Ristinge Klint

The Eemian deposits at Ristinge Klint are about 3.5 m thick and consist of the following conformable sequence: (1) a basal shell-free 'Shiny Clay' (Madsen, Nordmann & Hartz, 1908) of about 1 m thick, which has been interpreted as a freshwater deposit; (2) a 12 cm-thick 'Freshwater Sand' (Johnstrup, 1882; Madsen, Nordmann & Hartz, 1908); and (3) a marine greenish-grey clay (the Cyprina Clay) which is 2.32 m thick and relatively sandy at the base, becoming finer upwards. The Cyprina Clay contains a sparse mollusc fauna including shells of *Arctica* (formerly *Cyprina*) *islandica* (Kristensen *et al*. 2000). The Cyprina Clay is overlain by the 'White Sand' of Madsen, Nordmann & Hartz (1908), which may be a glaciofluvial deposit (Sjørring *et al*. 1982).

5. Materials and methods

The present study is based on the same samples used in Kristensen *et al*. (2000). Twenty-five samples were processed using standard palynological methods, except that hot acids, acetolysis, oxidation and alkali treatment were avoided to prevent damage to certain cysts. Previously dried samples were first weighed (2.9–3.9 g), and one or three (mostly three) *Lycopodium* tablets (batch no. 124961) were added to each sample to provide cyst concentrations. Samples were placed in 50 ml round-ended plastic centrifuge tubes and digested in cold 7 % HCl. Samples were then washed in H_2O by decanting in order to remove HCl and clay particles. This was followed by digestion in cold 40 % HF for 3 to 4 days, washing in H_2O, and treatment with cold 7 % HCl. Residues were stained with safranin-O, and a few were given brief ultrasound treatment prior to sieving. Residues were sieved at 10 μm and mounted on one or two microscope slides using glycerine jelly for counting. The remaining residue of selected samples was sieved at 20 μm and mounted for taxonomic analysis.

One slide from each sample was examined under a $\times$40 objective usually until at least 380 *in situ* dinoflagellate cysts had been counted. The remainder of the slide was then searched under lower magnification for rare specimens. Other categories of palynomorph were also enumerated. Results are plotted both as concentrations per gram dry weight of sediment (Fig. 3) and percentages of the total *in situ* dinoflagellate cysts (Fig. 4), and raw counts are given in Table 1.

Process length in *Operculodinium centrocarpum sensu* Wall & Dale (1966) and *Lingulodinium machaerophorum* is known to be influenced by several environmental parameters, but particularly salinity (e.g. R. I. Hallett, unpub. Ph.D. thesis, Univ. Westminster, 1999). To evaluate changes in average process length with time and hence palaeosalinity for morphotypes of *O. centrocarpum* (Fig. 6c–o) and *L. machaerophorum* (Fig. 6b), 20 specimens were measured per sample for each species (Fig. 5). Measurements were made under $\times$1250 magnification, and the average process length for each specimen was based on averaging the lengths of at least three processes at the periphery of the cyst, but ignoring any short processes that occur rarely on the cyst. The 20 measurements per sample for each species are expressed by the minimum, average, maximum and standard deviation (Fig. 5).

The wide range of process lengths for individual specimens, particularly in *L. machaerophorum*, introduces subjectivity in estimating average process length. Another source of uncertainty relates to the wide range in average process length between specimens for nearly every sample. Hence selected samples were subjected to repeat measurements, in order to check for reproducibility of results. These show that average process length per sample for *O. centrocarpum* is generally reproducible within about 0.5 μm or less. For *L. machaerophorum*, reproducibility is generally within about 1 μm. Central body diameter was not measured because crumpling of cysts made this unreliable, and because laboratory culturing experiments of *L. machaerophorum* suggest that central body size is not significantly affected by salinity (R. I. Hallett, unpub. Ph.D. thesis, Univ. Westminster, 1999).

Specimens were photographed using a Leica DC3 digital camera mounted on a Leica DMR microscope. Representative specimens are illustrated in Figures 6–12.

The microscope slide containing the holotype and paratype of *Spiniferites ristingensis* n. sp. is housed in the Invertebrate Section of the Department of Palaeobiology, Royal Ontario Museum, Toronto, Ontario, under the catalogue number ROMP 57997.

Table 1. Raw counts of dinoflagellate cysts and other palynomorphs recorded at Ristinge Klint, and associated sample data

Dinoflagellate cyst zones	Unzoned			RKDf 1				RKDf 2								RKDf 2b		RKDf 3							
Sample depth (cm)	284	264	244*	229	220	208	190	184	178	166	148	130	112	93	75	66	60	57	51	48	30	21	12	9	3
Dinoflagellate cysts																									
Spiniferites spp. undifferentiated				23	67	75	116	100	52	49	62	58	87	54	68	61	46	55	44	58	34	62	69	57	72
Lingulodinium machaerophorum				1		16	30	179	169	168	195	163	142	173	203	163	193	204	200	168	143	126	106	99	75
O. centrocarpum sensu Wall & Dale (1966)				+		19	10	23	24	28	50	60	76	60	33	46	46	62	92	83	80	105	92	106	102
O. centrocarpum – short processes					2	65	8	5	3		4	1	2	+	+	1	1	3	5	3	1	1	1	2	2
O. centrocarpum var. *cezare* s.l.						45	10		1		+		1												
Spiniferites bentorii						4	13	41	74	94	27	53	50	95	59	65	87	52	41	56	87	83	68	81	94
Bitectatodinium tepikiense							+			+															
Dubridinium spp.							+	2	14	4	12	6	+	1											
Quinquecuspis cf. *concreta*							1	1			+	2	+	+											
Brigantedinium? spp. indet.							4	14	9	4	9	6	1	1	+										
Selenopemphix quanta							5	1	2	4	6	2	1	3	+										
Xandarodinium xanthum							1			+		+	3	8	2			+	+						
Tectatodinium pellitum							1	2		1	1	4	1	1	1	+	1	2	+	1	3	+	1	2	+
Tuberculodinium vancampoae							+	5	9	11	4	4	12	13	18	48	31	13	18	9	19	22	29	36	23
Echinidinium zonneveldiae								+	1																
Echinidinium? sp. 2								1		1	1	+													
Polykrikos schwartzii cysts								1	10	10	3	4	+												
Pentapharsodinium dalei cysts								10	4		2	3	4	6	7	5	7	1	9		22	5	28	16	15
Spiniferites ristingensis sp. nov.								12	9	2	5	1		+	1	7	5	2	5	5	9	5	6	16	8
Stelladinium sp. 2									1																
Protoperidinium spp. indet.									1			9													
P. oblongum sensu Dale (1983, figs 11, 12 only)									2	6	2	3	+												
Quinquecuspis concreta									1	2	2		3	+	+										
Spiniferites mirabilis										1	8	9	15	6	5	11	6	6	6	6	2	3	7	7	5
Echinidinium? sp. 1											4	9	+												
Stelladinium sp. 1											+	1	+												
Lejeunecysta sp. 1 of Head *et al.* (2005)												1		+				+				+			
Spiniferites elongatus												+			+			+					1		
Achomosphaera andalousiensis																+	+	+	1				+	2	
Ataxiodinium choane																		+	1	+	+	1	1	+	+
Capisocysta lata																						2	1	4	1
Total heterotrophs	0	0	0	0	0	0	11	20	41	31	39	43	8	13	2	0	0	0	0	0	0	0	0	0	0
Total dinoflagellate cysts	0	0	0	24	69	224	199	397	386	385	397	399	398	421	397	407	423	400	422	389	400	415	410	428	397
Number of autotrophic taxa	0	0	0	3	2	6	9	9	9	9	11	11	10	10	11	11	11	13	12	10	11	12	14	13	12
Number of heterotrophic taxa	0	0	0	0	0	0	5	7	9	8	10	12	10	7	4	0	0	2	1	0	0	1	0	0	0
Number of all taxa	0	0	0	3	2	6	14	16	18	17	21	23	20	17	15	11	11	15	13	10	11	13	14	13	12
Other groups																									
Botryococcus	1	4		3	2	14	5	11	17	8	7	7	14	2		5			1						
Bisaccate pollen	32	55		225	260	426	638	203	604	250	308	211	310	128	116	99	147	83	128	65	21	20	10	22	9
Pediastrum	13	5		4	4	39	15	2	6	5	5	4	12	9	7	3	2	2	2	1	5	+	+	3	2
Reworked dinoflagellate cysts	26	37		25	178	188	190	59	40	42	45	42	89	49	51	32	54	28	48	24	23	22	14	45	24
Sigmopollis sp. of Head *et al.* (2005)	1	1		3	4	3	3	4	3		1	4	4	2	1	+		2	1		+	+	+	1	+
Zygnema-type						+						1													
Invertebrate mouthparts/appendages						1	13	3	5	3	5	1	9	2	2	+	+								
Cymatiosphaera spp.						1			+	2									+						
Tintinnid loricae						1	23	+	4	1	2	3	3	1	4	1	1	1			+	+	+		+
Invertebrate egg (scattered spinules)								2	1	+	7	18	2	1	+										
Invertebrate egg (long processes)									+																
Invertebrate egg (spongy wall)									+																
Invertebrate egg (fibroreticulate wall)										+															
Halodinium majus										+	+	2	4	1	1	+	+	+		+	+	+	+	+	1
Radiosperma corbiferum											+														
Mougeotia-type														+											
Sample data																									
Spike	600	600	600	600	600	600	207	198	290	260	192	135	121	35	130	171	94	168	195	260	55	138	186	293	216
Grams dry weight	3.3	3.4	3.5	3.1	3.3	3.7	3.0	3.7	3.0	3.1	3.3	3.3	3.0	3.1	3.5	3.6	3.0	3.9	3.7	2.9	2.9	3.8	3.1	3.6	3.8
No. *Lycopodium* tablets	3	3	3	3	3	3	1	3	3	3	3	3	1	1	3	3	1	3	3	3	1	3	3	3	3

*Barren sample. + Indicates the presence of a taxon recorded outside of the main count.

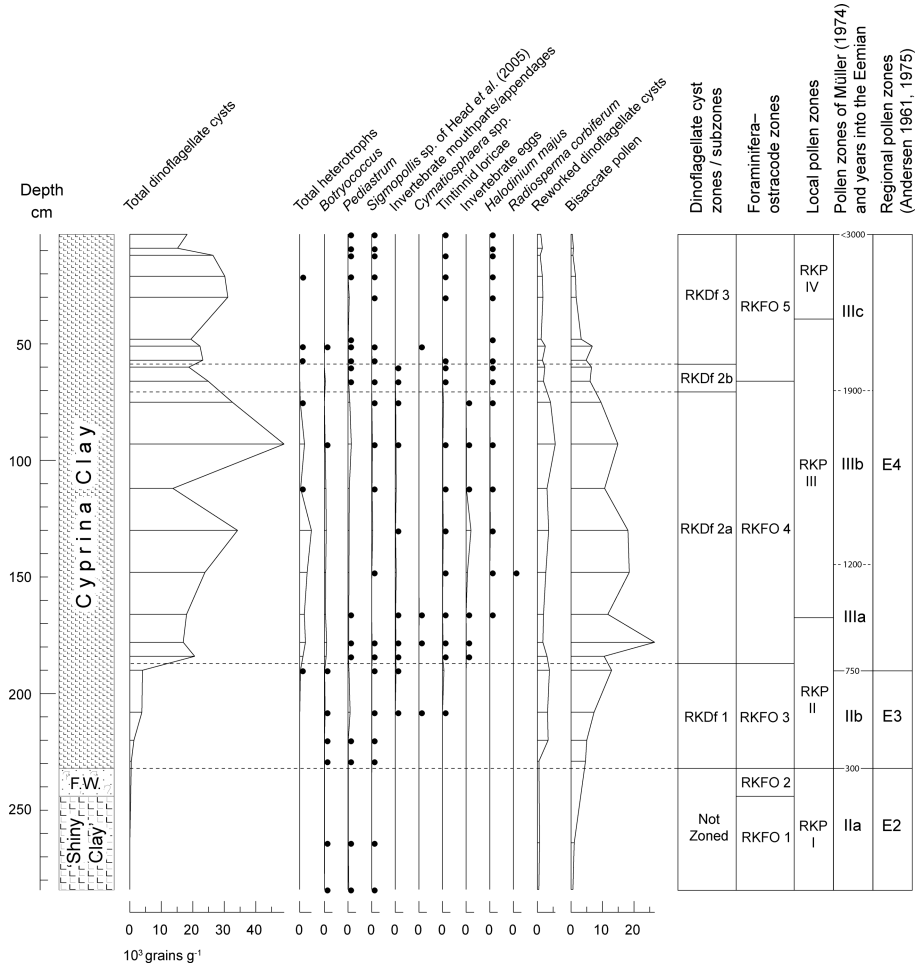

Figure 3. Concentrations (specimens per gram dry weight of sediment) of all palynomorph groups counted from the Eemian of Ristinge Klint. Solid dots indicate low concentrations (300 or less per gram). The dinoflagellate cyst assemblage biozones and subzones are from the present study, and the foraminifera–ostracode assemblage biozones and local pollen assemblage biozones are from Kristensen *et al*. (2000). The pollen zonation of Ristinge Klint is newly correlated to the pollen record at Bispingen in northern Germany (Müller, 1974). The ages of zonal boundaries are in years from the Saalian/Eemian boundary (Müller, 1974). The regional pollen zonation of Andersen (1961, 1975) is also included. Raw counts are listed in Table 1. F.W. = Freshwater Sand.

6. Age model

The age model is based on a correlation of the Ristinge Klint pollen stratigraphy provided by Kristensen *et al*. (2000) to the pollen zonation at Bispingen in northern Germany. The Bispingen record is calibrated by counting annual laminations in the sediments to provide a 'floating' chronology in which zonal boundaries are expressed in years after the Eemian onset (Müller, 1974). These pollen zones can be recognized in the Eemian across northern Europe (Head *et al*. 2005, fig. 5) and appear to be synchronous to within a few hundred years, at least for the early part of the Eemian (Zagwijn, 1996; Funder, Demidov & Yelovicheva, 2002).

Kristensen *et al*. (2000) drew the base of their zone RKP II with that of the Cyprina Clay (at 232 cm) by interpolating between a sample 15 cm above the base of the Cyprina Clay, and a sample 12 cm below it. The rise of *Quercus* defines the base of zone RKP II and it had already reached a maximum development in the lowest sample of the Cyprina Clay at 15 cm above its base. To establish whether the base of the Cyprina Clay indeed represents a rise in *Quercus*, as assumed by Kristensen *et al*. (2000), or whether peak abundances extend to the base (which might then indicate a stratigraphic gap associated with the Freshwater Sand), a sample at 229 cm was counted for pollen as it occurs just 3 cm above the base of the Cyprina Clay. This sample contains about 35 % *Quercus*, which is intermediate between the samples immediately above and below it (45 % and about 10 %, respectively), and so confirms that the base of the Cyprina Clay corresponds to a rise in *Quercus*. The base of the Cyprina Clay can therefore be correlated to the IIa/IIb zonal boundary at Bispingen which is dated at about 300 years into the Eemian (Müller, 1974). This agrees with the age model of Kristensen *et al*. (2000).

The IIb/IIIa zonal boundary of Müller (1974) is characterized by relatively low but rapidly rising values of *Corylus* pollen as well as of *Alnus*. The *Alnus* rise

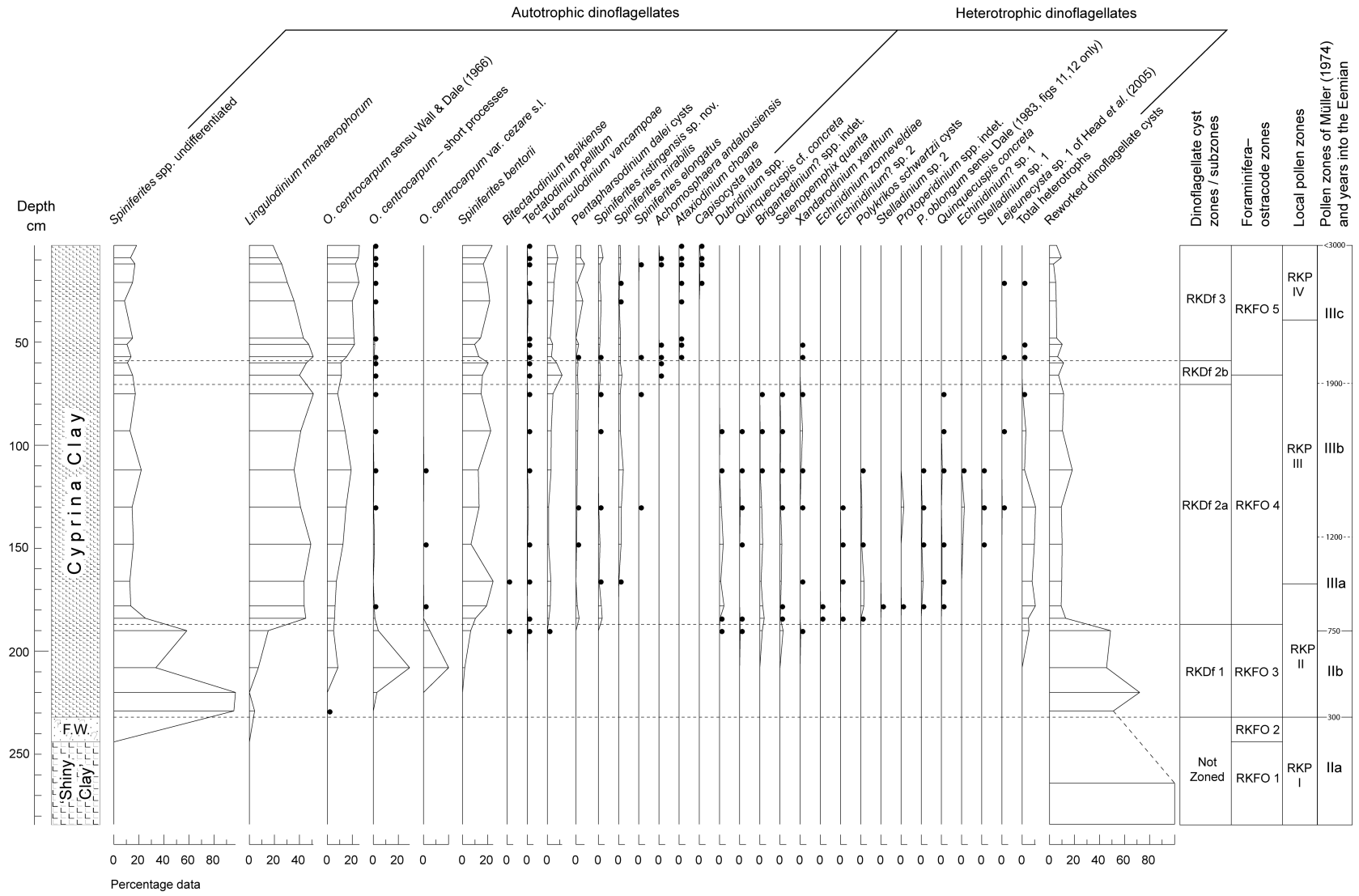

Figure 4. Relative abundance of dinoflagellate cysts from the Eemian of Ristinge Klint. Solid dots indicate rare occurrences (1 % or less). Reworked dinoflagellate cysts are expressed as a proportion of the *in situ* dinoflagellate cysts. The dinoflagellate cyst assemblage biozones and subzones, the foraminifera–ostracode assemblage biozones, pollen assemblage biozones, and ages of zonal boundaries are as for Figure 3.

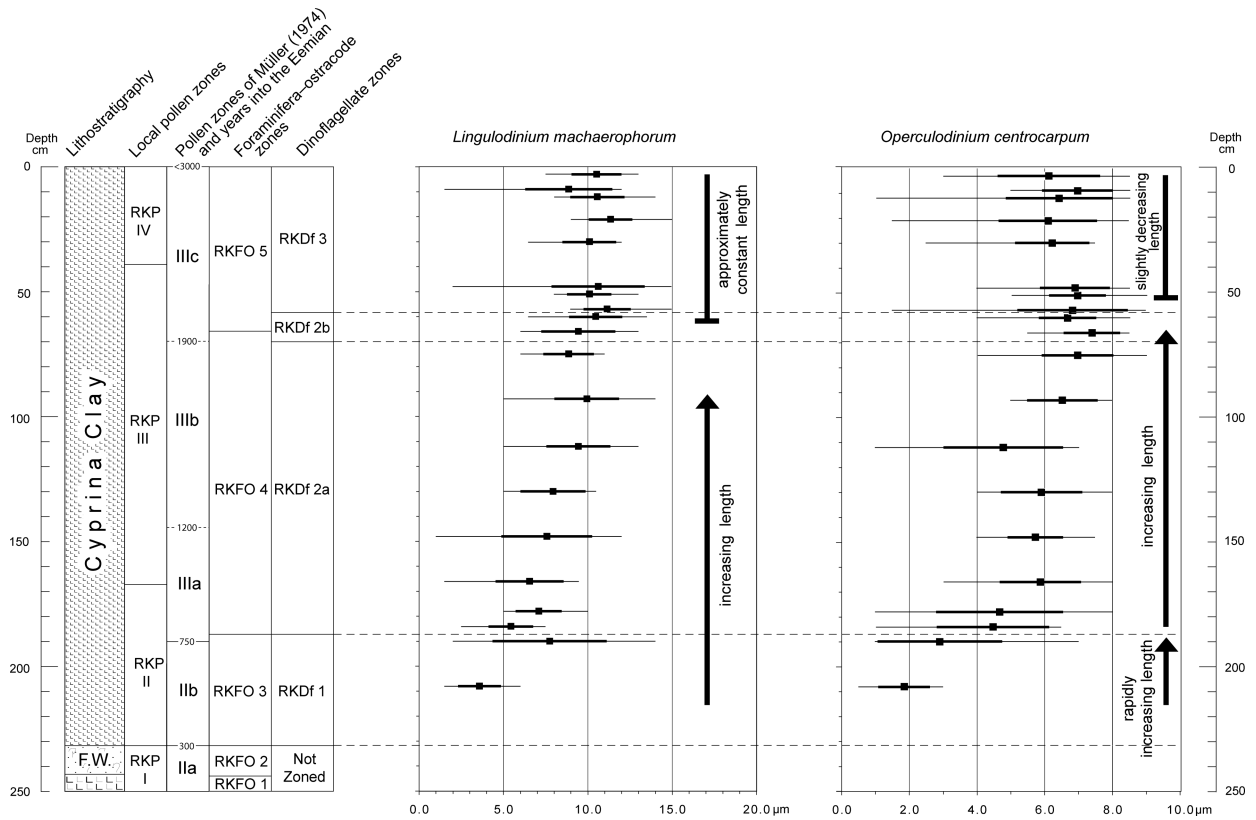

Figure 5. Process length for specimens of *Lingulodinium machaerophorum* and *Operculodinium centrocarpum* at Ristinge Klint, showing salinity-driven variation through the Cyprina Clay. A total of 20 specimens were measured per sample for each species. A thin line represents the total range in average process length, a thicker line the standard deviation, and the solid square the average process length for that sample. The dinoflagellate cyst assemblage biozones and subzones, the foraminifera–ostracode assemblage biozones, pollen assemblage biozones, and ages of zonal boundaries are as for Figure 3.

is not detected in the Ristinge Klint pollen record, but the *Corylus* rise is well developed. Accordingly, the IIb/IIIa zonal boundary can be placed at 190 cm at Ristinge Klint, at the earliest significant rise of *Corylus*. The IIb/IIIa zonal boundary at Bispingen is dated at about 750 years into the Eemian (Müller, 1974). This observation differs in detail from the age model of Kristensen *et al*. (2000), which places the boundary about 25 cm higher in the section.

The IIIa/IIIb zonal boundary of Müller (1974) is based on the attainment of nearly peak values of *Corylus* as well as a significant decline in *Pinus* (see also Field, Huntley & Müller, 1994). At Ristinge Klint, this boundary is placed only approximately because the *Corylus* peak is less well defined than at Bispingen and the *Pinus* decline is not present. The boundary, placed at *c*. 148 cm at Ristinge Klint, coincides with an age of 1200 years into the Eemian (Müller, 1974). Kristensen

Figure 6. Dinoflagellate cysts from the Eemian of Ristinge Klint. Image (a) in interference contrast illumination, the others bright field. Various magnifications. Max. dia. = maximum diameter. (a) cyst of *Polykrikos schwartzii* Bütschli. Lateral view at middle focus; length 76 μm; depth 178 cm, slide 2, EF O37/1. (b) *Lingulodinium machaerophorum* (Deflandre & Cookson). Dorsal view at upper focus; central body length 42 μm; depth 57 cm, slide 1, EF H48/1. (c, d) *Operculodinium centrocarpum sensu* Wall & Dale (1966). Dorsal view at upper and middle foci; central body length 40 μm; depth 57 cm, slide 1, EF P12/1. (e–g) *Operculodinium centrocarpum*–short processes; antapical view at upper, middle and lower foci; note faintly granulate surface and predominantly cylindrical processes with minutely flared distal margins; central body max. dia. 31 μm; depth 93 cm, slide II >10 μm, EF M47/4. (h–j) *Operculodinium centrocarpum* form B of de Vernal, Goyette & Rodrigues (1989; also known as *Operculodinium centrocarpum* Arctic morphotype in de Vernal *et al*. 2001). Ventral view at upper through middle foci, showing sparsely distributed processes, often conical, and tapering to acuminate or minutely expanded tips; max. dia. central body 34 μm; depth 208 cm, slide 1, EF N39/4. (k–o) *Operculodinium centrocarpum* var. *cezare* de Vernal, Goyette & Rodrigues, 1989 ex de Vernal, herein. Note dense processes, some almost hairlike. (k–m) Dorsal view at upper, slightly lower, and middle foci; central body length 37 μm; depth 208 cm, slide 1, EF R18/1. (n, o) View uncertain at upper and middle foci; central body max. dia. 37 μm; depth 208 cm, slide 1, EF U43/2. (p–s) *Ataxiodinium choane* Reid, showing range in development of periblast invagination. (p–r) Right lateral view at upper, middle, and lower foci; central body length 35 μm; depth 9 cm, slide 1, EF G25/2. (s) Dorsal view of dorsal surface; central body length 34 μm; depth 9 cm, slide 1, EF O10/2 (see also Fig. 7a, b).

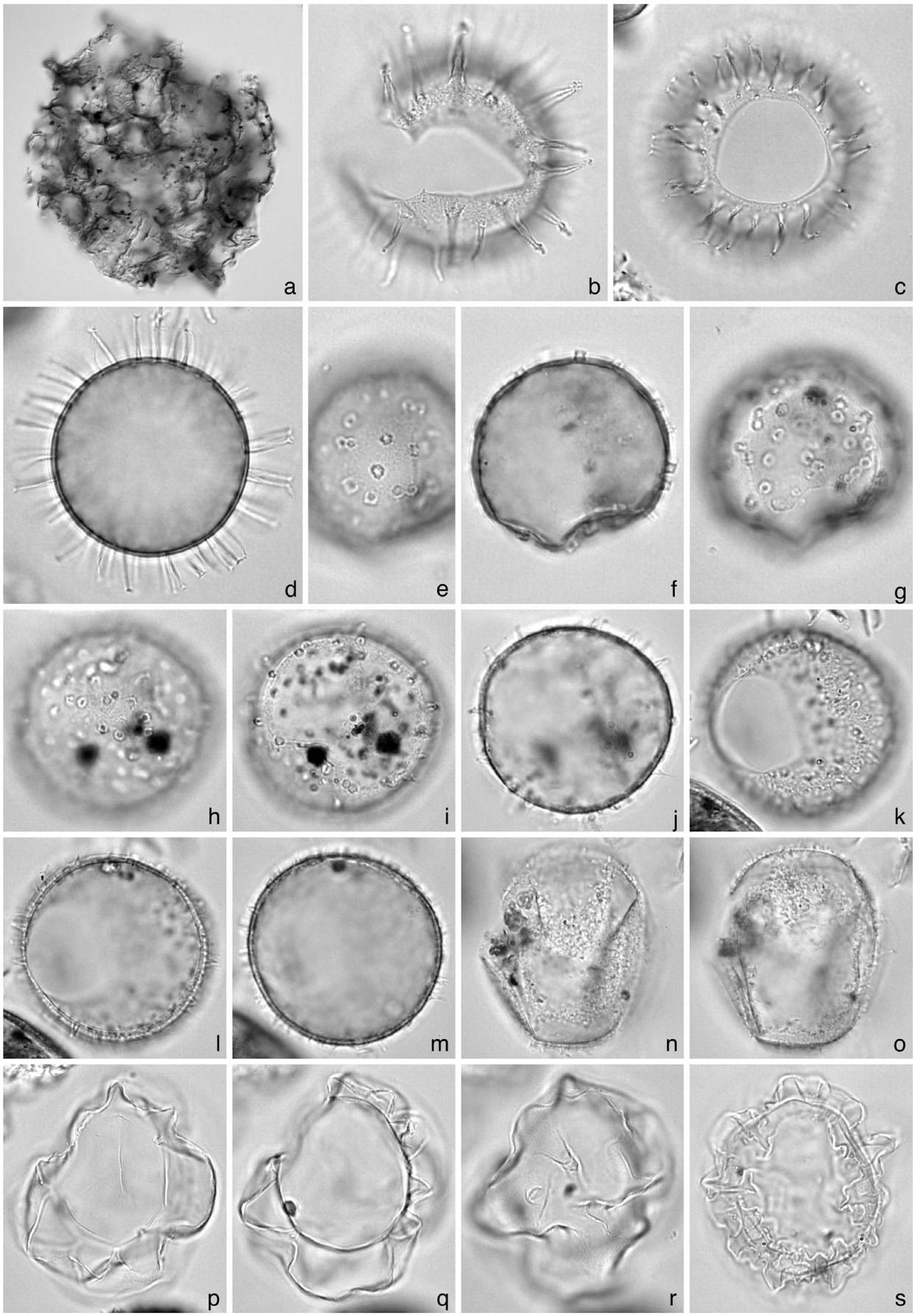

Figure 6. For legend see previous page.

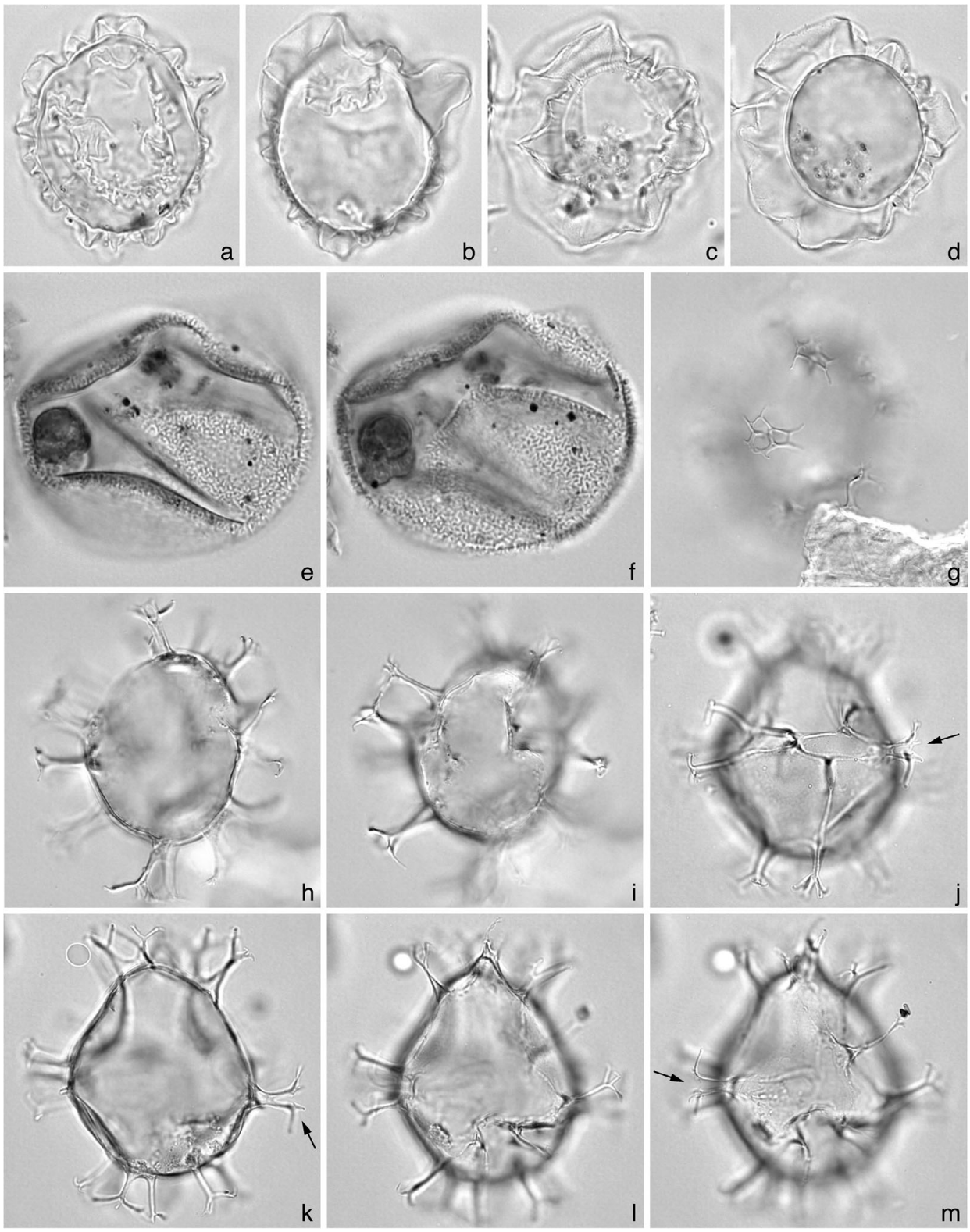

Figure 7. Dinoflagellate cysts from the Eemian of Ristinge Klint. Images are in bright field (a–f, j–m) and interference contrast (g–i) illumination. Various magnifications. Max. dia. = maximum diameter. (a–d) *Ataxiodinium choane* Reid, showing range in development of periblast invagination. (a, b) dorsal view at middle and lower foci; central body length 34 μm; depth 9 cm, slide 1, EF O10/2 (see also Fig. 6s). (c, d) dorsal view at upper and middle foci; central body length 33 μm; depth 9 cm, slide 1, EF N45/1. (e, f) *Bitectatodinium tepikiense* Wilson. Polar view at upper and middle foci showing diagnostic wall ornament; central body max. dia. (excluding luxuria) 45 μm; depth 166 cm, slide 1, EF M18/3. (g–i) *Achomosphaera andalousiensis* Jan du Chêne. Right-lateral view at upper, middle and lower foci, showing characteristic fenestrate distal process platform in (i); central body length 47 μm; depth 57 cm, slide 1, EF M48/1. (j–m) *Spiniferites bentorii* (Rossignol). Dorsal view at successively lower foci, showing characteristic morphology of cingular processes (marked by arrows); central body length 57 μm; depth 57 cm, slide 1, EF U22/0.

et al. (2000) did not identify this boundary in their zonation of Ristinge Klint.

The IIIb/IIIc zonal boundary of Müller (1974) is based on the decline of *Corylus* following its peak within zone IIIb. The placement of this boundary at *c*. 70 cm at Ristinge Klint is approximate, for reasons given above. Kristensen *et al*. (2000) did not identify this boundary in their zonation of Ristinge Klint.

The IIIc/IVa zonal boundary of Müller (1974) is based on the rapid rise to dominance of *Carpinus*. At the same time, there is a more gradual increase in *Picea* and a gradual decline in *Corylus* across the boundary. The present interpretation does not recognize Müller's zone IV in the Ristinge Klint pollen record. However, increasing values of *Carpinus* and *Picea* (although with *Corylus* nevertheless more abundant) recorded by Kristensen *et al*. (2000) in their highest sample suggest that it is not far from the IIIc/IVa zonal boundary. The IIIc/IVa zonal boundary at Bispingen is dated at about 3000 years into the Eemian (Müller, 1974), and the highest sample at Ristinge Klint is therefore a little less than this. This interpretation differs from that of Kristensen *et al*. (2000) who assigned an age of *c*. 3400 years to the top of the sequence.

7. Palynomorph assemblages at Ristinge Klint

Palynomorphs occur in all samples with the exception of a sample at 244 cm, which is barren. The spore and pollen assemblages are described by Kristensen *et al*. (2000). *In situ* dinoflagellate cysts occur from 229 cm to the top of the section, and are represented by at least 29 taxa. Cysts of autotrophic dinoflagellates are well preserved throughout. The heterotrophic dinoflagellate cysts are mostly restricted to an interval between 190 and 75 cm (Table 1), and their preservation varies from good to poor. Cysts of heterotrophic dinoflagellates are preferentially susceptible to oxidation, and their preservation can be affected by oxidizing bottom waters during deposition and also by post-depositional (weathering) processes. Woody tissues, cuticle, pollen and spores are abundant in the interval below 75 cm, indicating proximity to shore.

8. Reworked dinoflagellate cysts

Reworked dinoflagellate cysts occur throughout the examined interval at Ristinge Klint, and constitute between about 10 and 60 % of the dinoflagellate cysts for most of the samples in the marine Cyprina Clay (Figs 3, 4). The identifiable taxa are mostly of Paleogene age (Stover *et al*. 1996; Williams *et al*. 2004) and include *Diphyes colligerum* (Late Paleocene through Early Oligocene); the Eocene species *Eatonicysta ursulae* (Early and Middle Eocene) and *Areosphaeridium diktyoplokum* (Early Eocene through earliest Oligocene); and the Eocene–Oligocene species *Enneadocysta arcuata* (Middle Eocene through Early Oligocene), *Chiropteridium lobospinosum* (Late Eocene through Oligocene), *Membranophoridium aspinatum* (Late Eocene through Late Oligocene), *Wetzeliella symmetrica* (Late Eocene through Late Oligocene), and *Wetzeliella* spp. (Early Eocene through Oligocene). Mesozoic dinoflagellate cysts are represented in fewer numbers throughout the sequence and include, for example, representatives of the Cretaceous genus *Odontochitina*. Differential preservation was often

Figure 8. Dinoflagellate cysts from the Eemian of Ristinge Klint. All images in bright field illumination. Various magnifications. (a, b) *Spiniferites mirabilis* (Rossignol). Ventral view at middle and lower foci; central body length 47 μm; depth 21 cm, slide 1, EF P20/0. (c–l) *Spiniferites ristingensis* sp. nov. showing central body with minutely and densely distributed blisters and hollow undulations in the outer wall layer, and granulate membranous processes. (c–g) Holotype; ventral view at successively lower foci, including (d) close-up of bilayered central body wall, and arrow marking bilayered membranous process stem, and (g) low sutural crest along margin of archeopyle; central body length 42 μm; depth 57 cm, slide 1, EF P8/1; ROMP 57997. (h–l) Paratype; left lateral view at successively lower foci, with (k) showing spine-like process at apex marked by arrow; central body length 45 μm; depth 57 cm, slide 1, EF H49/2; ROMP 57997.

Figure 9. Dinoflagellate cysts from the Eemian of Ristinge Klint. Images are in (a, b, e–k, q–t) bright field, (c, d, l–n) interference contrast, and (o, p) phase contrast illumination. Various magnifications. Max. dia. = maximum diameter. (a–d) Cysts of *Gonyaulax baltica* Ellegaard, Lewis & Harding showing processes of reduced length. (a, b) Apical view at high and middle focus; central body max. dia. 47 μm; depth 229 cm, slide 1, EF K18/2. (c, d) Dorsal view at middle and slightly lower focus, showing intergonal as well as gonal processes and well-developed membrane between two antapical processes; central body max. dia. 41 μm; depth 220 cm, slide 1, EF T26/1. (e–h) *Spiniferites* sp. 1, a common species in most samples. (e, f) Ventral view at upper and middle foci; central body length 38 μm; depth 112 cm, slide 1, EF Q34/2. (g, h) ventral view at upper and lower foci; central body length 35 μm; depth 148 cm, slide 5, EF R17/0. (i, j) *Tectatodinium pellitum* Wall. Dorsal view at upper and middle foci; central body length (incl. luxuria) 45 μm; depth 21 cm, slide 1, EF H14/4. (k) *Tuberculodinium vancampoae* (Rossignol). Apertural view at middle focus; maximum diameter 85 μm; depth 60 cm, slide 1, EF P20/0. (l–p) *Capisocysta lata* Head. Apical view of (l–n) upper, middle and lower foci showing posterior sulcal (ps) and other hypocystal plates, and (o, p) a close-up of the posterior sulcal plate showing the diagnostic shape of this species; epicyst max. dia 48 μm; depth 21 cm, slide 1, EF U29/1. (q–t) cyst of *Pentapharsodinium dalei* Indelicato & Loeblich. Unknown view at upper through lower foci showing unornamented wall and heterogenous process morphology; depth 93 cm, slide >10 μm, II, EF T30/2.

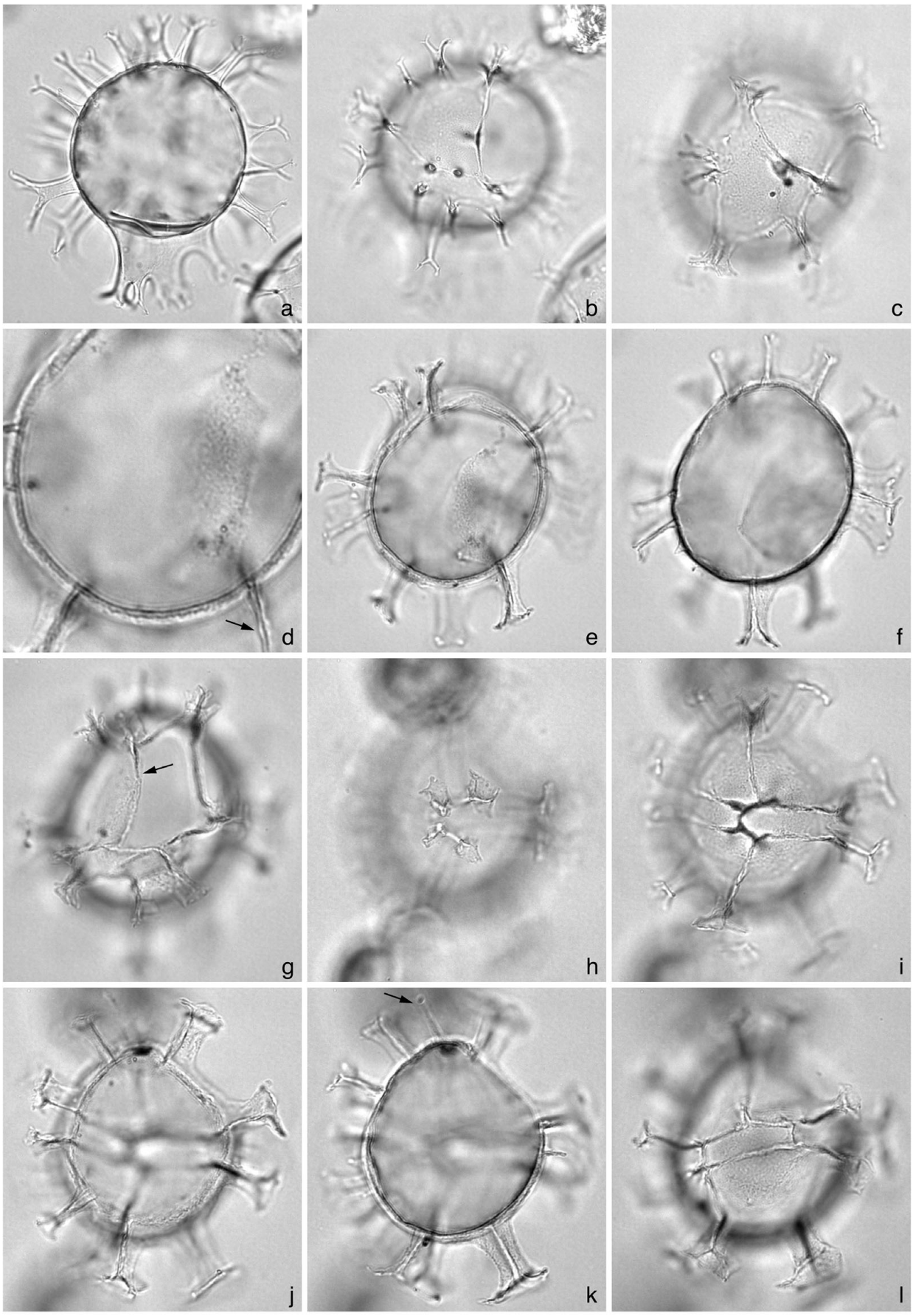

Figure 8. For legend see previous page.

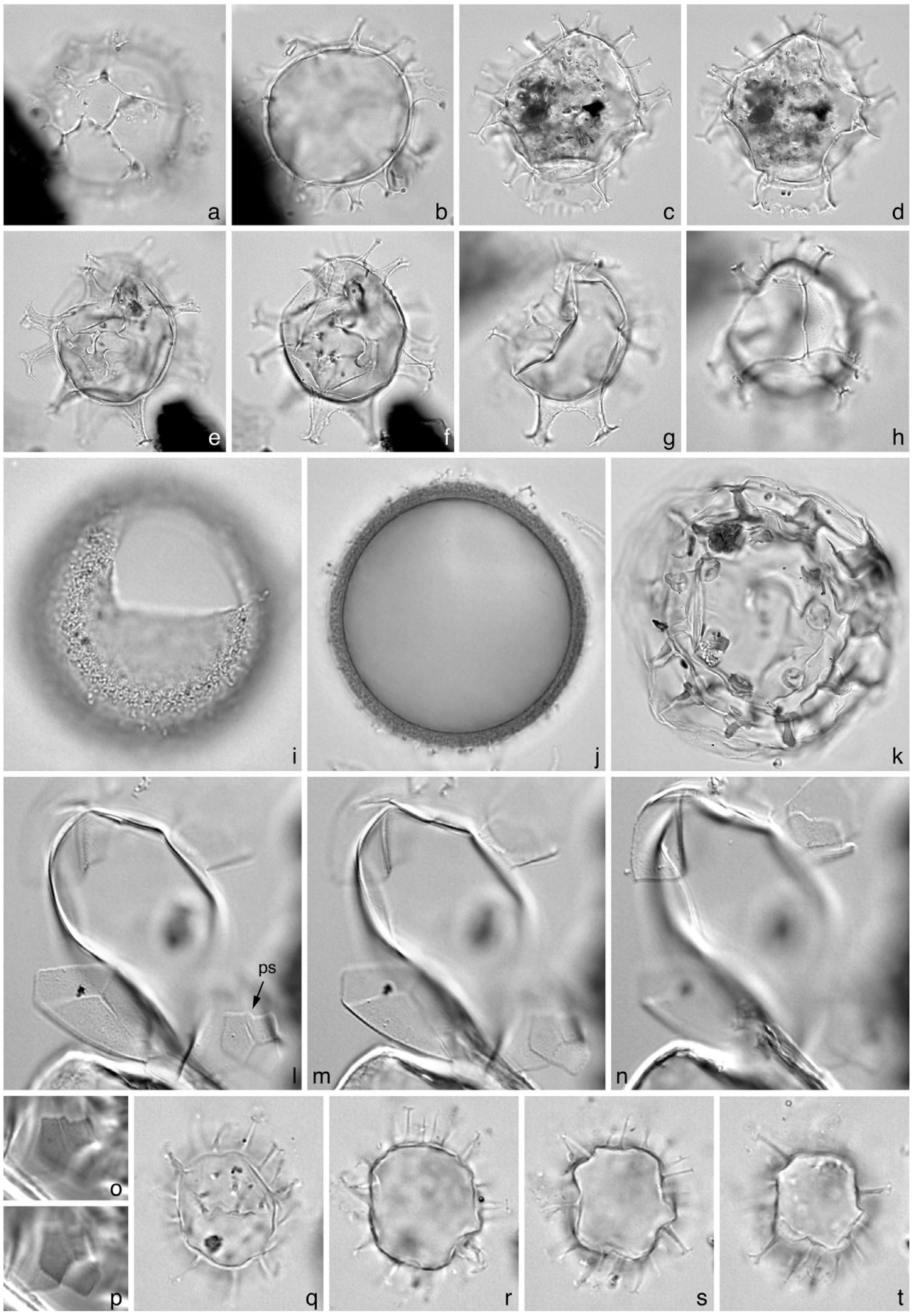

Figure 9. For legend see page 11.

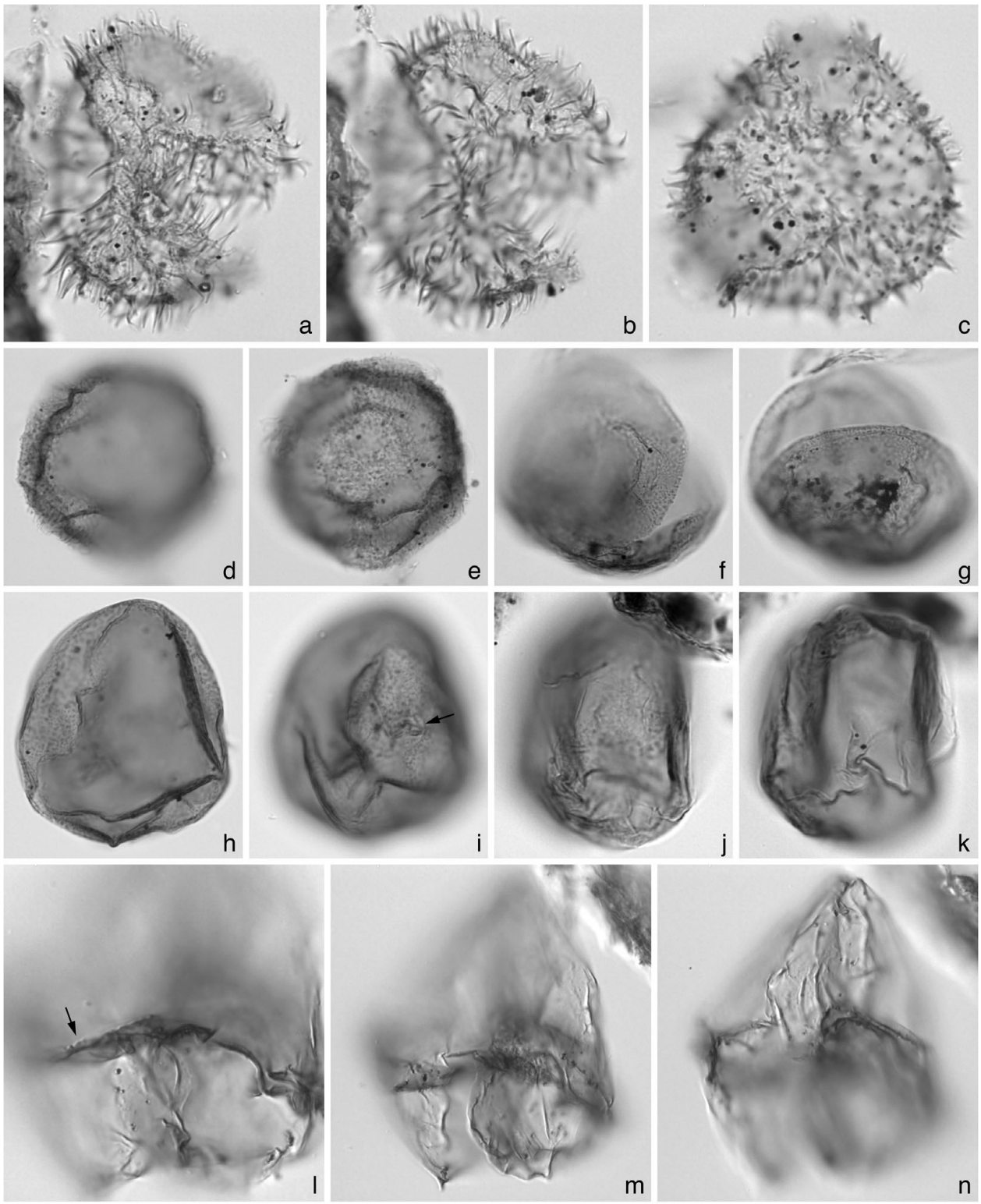

Figure 10. Dinoflagellate cysts from the Eemian of Ristinge Klint. Images are in (a–k) bright field, and (l–n) interference contrast illumination. Various magnifications. Max. dia. = maximum diameter. (a–c) *Echinidinium*? sp. 1. (a, b) Unknown view at upper and lower foci showing simple apertural split; central body max. dia. 47 μm; depth 112 cm, slide 3, EF G7/0. (c) Unknown view at middle focus; central body max. dia. 35 μm; depth 130 cm, slide 2, EF K45/0. (d, e) *Echinidinium*? sp. 2. Unknown view at upper and middle foci; central body max. dia. 38 μm; depth 130 cm, slide 1, EF Q23/4. (f–i) *Dubridinium* sp. 1. (f, g) Apical? view at upper and lower foci showing theropylic archeopyle along cingular margin; maximum diameter 48 μm; depth 130 cm, slide 1, EF L38/0. (h, i) Antapical? view at upper and lower foci, with apical pore complex in (i) shown by arrow; maximum diameter 48 μm; depth 112 cm, slide 3, EF V36/3. (j, k) *Dubridinium* sp. 2. Unknown view at upper and middle foci showing loosely appressed periblast; maximum diameter 41 μm; depth 148 cm, slide 1, EF S14/1. *Dubridinium* spp. 1 and 2 are grouped as *Dubridinium* spp. in the counts. (l–n) *Lejeunecysta* sp. 1 of Head *et al*. (2005). Dorsal view at upper, middle and lower foci, with (1) close-up showing irregularly denticulate cingular margins; length 71 μm; depth 130 cm, slide 1, EF Q34/2.

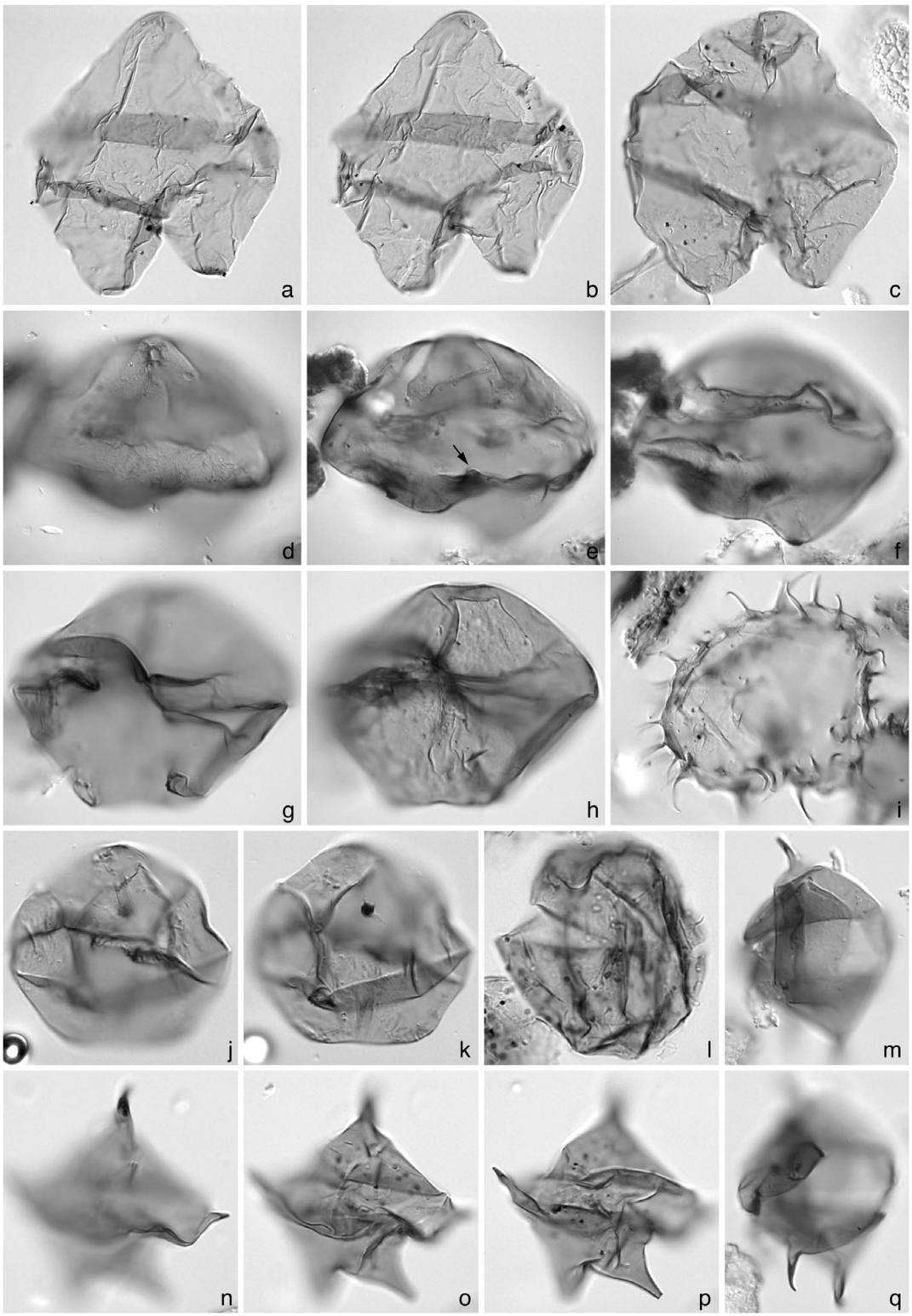

Figure 11. Dinoflagellate cysts from the Eemian of Ristinge Klint. Images are in (a–k, m–q) interference contrast illumination, and (l) bright field. Various magnifications. Max. dia. = maximum diameter. (a–c) *Protoperidinium oblongum sensu* Dale (1983, figs 11 and 12 only). (a, b) Ventral view at upper and lower foci; length 74 μm; depth 166 cm, slide 1, EF G36/4. (c) Ventral? view at middle focus; length 69 μm; depth 112 cm, slide 3, EF S9/0. (d–h) *Quinquecuspis concreta* (Reid). (d–f) Ventral view at upper, middle and lower foci; width 80 μm; depth 112 cm, slide 3, EF N50/0. (g, h) Ventral view at upper and lower foci; length 57 μm; depth 112 cm, slide 3, EF O27/4. (i) *Selenopemphix quanta* (Bradford). Apical view at middle focus; central body max. dia., 62 μm; depth 112 cm, slide 3, EF R47/0. (j, k) *Quinquecuspis* sp. cf. *Q. concreta* (Reid). Ventral? view at upper and lower foci; length 45 μm; depth 93 cm, slide II, EF D9/2. (l) *Echinidinium zonneveldiae* Head. Equatorial view at middle focus of specimen opened along theropylic (cingular) archeopyle; central body length 39 μm; depth 184 cm, slide 3, EF S40/0. (m–q) *Stelladinium* sp. 1. (m, q) left lateral view at upper and middle foci; length 52 μm; depth 112 cm, slide 3, EF N9/3. (n–p) dorsal view at upper, middle and lower foci, showing operculum slightly displaced and antapical horn tips broken off; length 53 μm; depth 112 cm, slide 3, EF O40/4.

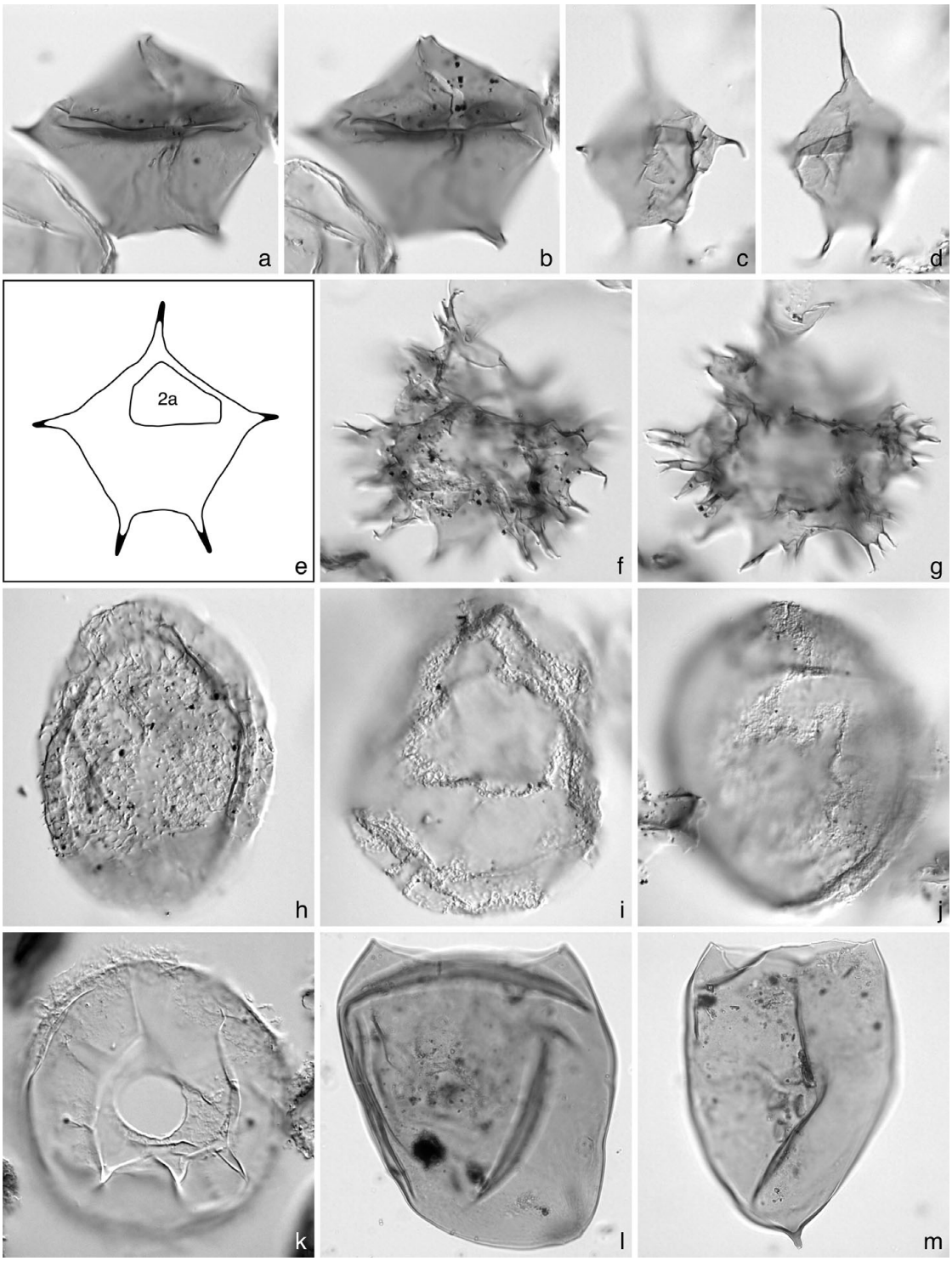

Figure 12. Dinoflagellate cysts from the Eemian of Ristinge Klint. Images are in (a–d, f–k) interference contrast illumination, and (l, m) bright field. Various magnifications. (a, b, e) *Stelladinium* sp. 1. (a, b) Ventral view of specimen with apical and antapical horn tips broken off, at (a) upper focus showing narrow sulcus, and (b) lower focus showing slightly displaced operculum; length 49 μm; depth 112 cm, slide 3, EF S35/0. (e) Sketch interpreted from numerous mostly incomplete specimens showing large asymmetrically shaped 2a archeopyle offset to the right. (c, d) *Stelladinium* sp. 2. Dorsoventral view at upper and lower foci showing exceptionally long apical and antapical horns; length 59 μm; depth 178 cm, slide 2, EF S22/1. (f, g) *Xandarodinium xanthum* Reid. Ventral? view at upper and lower foci; length 68 μm; depth 112 cm, slide 3, EF U46/0. (h) Invertebrate egg (scattered spinules). Lateral view at middle focus; length 75 μm; depth 130 cm, slide 2, EF V10/2. (i) Invertebrate egg (fibroreticulate wall). Lateral view at middle focus; length 78 μm; depth 166 cm, slide 1, EF K18/2. (j) Invertebrate egg (spongy wall). Lateral view at middle focus; length 78 μm; depth 178 cm, slide 2, EF K32/3. (k) *Hallodinium majus* Bujak. External polar view; central body max. dia. 65 μm; depth 148 cm, slide 5, EF R16/1. (l) Tintinnid lorica sp. 1. Lateral view at middle focus showing striae radiating from base; length 135 μm; depth 190 cm, slide >25 μm, 1, EF S35/2. (m) Tintinnid lorica sp. 2. Lateral view at middle focus showing smooth wall; length 117 μm; depth 75 cm, slide 1, EF G23/2.

used to identify reworked specimens belonging to the long-ranging genera *Spiniferites* and *Achomosphaera*. Dinoflagellate cysts having exclusively Neogene ranges were not seen.

9. Local dinoflagellate cyst zonation

The distribution of palynomorphs (relative abundances and concentrations) at Ristinge Klint has been used visually to subdivide the Eemian sequence into four local biostratigraphic units: an unzoned interval at the base, succeeded by three local dinoflagellate cyst assemblage biozones RKDf 1, RKDf 2 (subdivided into subzones RKDf 2a and RKDf 2b) and RKDf 3 (Figs 3–5). These units are as follows.

9.a. Unzoned interval (284–232 cm)

This interval represents the 'Shiny Clay' and 'Freshwater Sand' and is characterized by an absence of marine dinoflagellate cysts. *In situ* terrestrial palynomorphs, freshwater algae (e.g. *Pediastrum*) and reworked dinoflagellates are present in low concentrations at 284 cm and 264 cm from the Shiny Clay. A sample at 244 cm from the Freshwater Sand is barren of palynomorphs.

The interval corresponds to foraminifera/ostracode zones RKFO 1 ('Shiny Clay') and RKFO 2 ('Freshwater Sand'), and to local pollen assemblage zone RKP I *Betula–Pinus–Alnus* (Kristensen *et al*. 2000), which is correlated to pollen zone IIa of Müller (1974) and regional pollen zone E2 of Andersen (1961, 1975). The age is between about 100 and 300 years after the Eemian onset (Fig. 3).

9.b. RKDf 1 (232–187 cm) *Spiniferites* spp.–*Operculodinium centrocarpum* Assemblage Biozone

This zone represents the lowest part of the Cyprina Clay. The lowest occurrence of marine dinoflagellates (*Operculodinium centrocarpum sensu* Wall & Dale, 1966, *Lingulodinium machaerophorum,* and the cysts of *Gonyaulax baltica* which are included within *Spiniferites* spp. undifferentiated in Fig. 4), at 229 m, defines the base of this zone, which is assumed to extend to the base of the Cyprina Clay at 232 cm. The zone is characterized by low concentrations of cysts and low species richness (although diversity increases upwards), and by the co-dominance of *Gonyaulax baltica* cysts (Fig. 9a–d) and morphotypes of *Operculodinium centrocarpum* (Fig. 6c–o). The middle part of the zone has the lowest occurrence of *Spiniferites bentorii* (Fig. 7j–m), and also contains characteristic peaks of *Operculodinium centrocarpum*–short processes (Fig. 6e–g) and *Operculodinium centrocarpum* var. *cezare s.l.* (Fig. 6k–o; Appendix 1). Several dinoflagellate cyst species have their lowest occurrence in the uppermost sample at 190 cm.

Zone RKDf 1 corresponds to foraminifera/ostracode zone RKFO 3, and in part to local pollen assemblage zone RKP II *Quercus–Ulmus* (Kristensen *et al*. 2000). Zone RKDf 1 is also correlated to pollen zone IIb of Müller (1974) and regional pollen zone E3 of Andersen (1961, 1975). The base of zone RKDf 1 is dated at about 300 years after the Eemian onset (Fig. 3).

9.c. RKDf 2 (187–58.5 cm) *Lingulodinium machaerophorum* Assemblage Biozone

Zone RKDf 2 represents the middle part of the Cyprina Clay at Ristinge Klint. The base is sharply defined by an increase in total cyst concentration, a drop in the relative abundance of reworked dinoflagellates, the abrupt rise to dominance of *Lingulodinium machaerophorum* (Fig. 6b), and lowest occurrence of several taxa including the dinoflagellate cysts *Spiniferites ristingensis* sp. nov. (Fig. 8c–l), *Echinidinium zonneveldiae* (Fig. 11l) and *Polykrikos schwartzii* (Fig. 6a), and the incertae sedis palynomorph *Halodinium majus* (Fig. 12k). Invertebrate mouthparts/appendages have their highest occurrence at the top of this zone.

The zone is divided into two subzones. RKDf 2a (187–70.5 cm) is characterized by the consistent presence of cysts of heterotrophic dinoflagellates, most species of which range no higher than this subzone. Invertebrate eggs are restricted to this subzone. RKDf 2b (70.5–58.5 cm) is characterized by an absence of cysts of heterotrophic dinoflagellates, by elevated numbers of *Tuberculodinium vancampoae* (Fig. 9k), and by the lowest occurrence of *Achomosphaera andalousiensis* (Fig. 7g–i) at the base of this subzone.

Subzone RKDf 2a corresponds to foraminiferal/ostracode zone RKFO 4 (pars), and local pollen assemblage zones RKP II *Quercus–Ulmus* (pars) and RKP III *Corylus–Quercus* (pars) (Kristensen *et al*. 2000). Subzone RKDf 2a is also correlated approximately to pollen zones IIIa and IIIb of Müller (1974) and regional pollen zone E4 (pars) of Andersen (1961, 1975). The base of the subzone is dated at about 750 years after the Eemian onset (Fig. 3). Subzone RKDf 2b corresponds to the upper part of foraminiferal/ostracode zone RKFO 4 and the lower part of RKFO 5, and to local pollen assemblage zone RKP III *Corylus–Quercus* (pars) (Kristensen *et al*. 2000). Subzone RKDf 2b is also correlated approximately to the basal part of pollen zone IIIc of Müller (1974) and regional pollen zone E4 (pars) of Andersen (1961, 1975). The base of the subzone is dated at *c*. 1900 years after the Eemian onset (Fig. 3).

9.d. RKDf 3 (58.5–3 cm) *Ataxiodinium choane* Assemblage Biozone

This zone represents the highest part of the Cyprina Clay at Ristinge Klint. Its base is defined by the lowest occurrence of *Ataxiodinium choane* (Figs 6p–8,

7a–d), by a rise in abundance of *Operculodinium centrocarpum sensu* Wall & Dale, 1966 (Fig. 6c, d), and by a decline in *Lingulodinium machaerophorum* (Fig. 6b) above the lowest sample. The zone is also characterized by a slight increase in *Pentapharsodinium dalei* cysts (Fig. 9q–t). Cysts of heterotrophic dinoflagellates are rare, but those of autotrophic dinoflagellates have their highest species richness (10–14 taxa) within this zone (Table 1). *Capisocysta lata* (Fig. 9l–p) has its lowest occurrence within this zone.

Zone RKDf 3 corresponds to foraminiferal/ostracode zone RKFO 5 (pars), and to local pollen assemblage zones RKP III *Corylus–Quercus* (pars) and RKP IV *Pinus–Picea–Corylus* (Kristensen *et al*. 2000). Zone RKDf 3 is also correlated to pollen zone IIIc (pars) of Müller (1974) and regional pollen zone E4 (pars) of Andersen (1961, 1975). The zone approximately extends from *c*. 1900 to *c*. 3000 years after the Eemian onset (Fig. 3).

10. Hydrographic history

The hydrographic history at Ristinge Klint has been reconstructed by integrating the ecological signal of the dinoflagellate cysts, which reflect conditions in the upper part of the water column, with the benthic ecological signal from ostracodes and foraminifera as reported in Kristensen *et al*. (2000).

10.a. Unzoned interval (284–232 cm), *c*. 100–300 years into Eemian

The absence of *in situ* marine dinoflagellate cysts, including those tolerant of low salinities, and the presence of freshwater algae (e.g. *Pediastrum, Botryococcus* and *Sigmopollis*), indicate that the Shiny Clay was deposited in a freshwater environment. This supports the lacustrine interpretation of Sjørring *et al*. (1982). No ostracodes or foraminifera were found in the Shiny Clay (Kristensen *et al*. 2000). The low concentrations of palynomorphs (Fig. 3) suggest rapid deposition of this clay.

No palynomorphs were found in the overlying 'Freshwater Sand', probably owing to lack of preservation. This unit has been interpreted as a lacustrine deposit (Sjørring *et al*. 1982), and evidence from ostracodes and oospores of *Chara* suggests a freshwater to marginal marine environment (Kristensen *et al*. 2000).

10.b. RKDf 1 (232–187 cm) *Spiniferites* spp.–*Operculodinium centrocarpum* Assemblage Biozone, *c*. 300–750 years into Eemian

The lowest occurrence of marine dinoflagellates at 229 cm, which represents the lowest sample examined for the Cyprina Clay and is 3 cm above its base, effectively places the beginning of the marine ingression at the base of the Cyprina Clay. The base of zone RKDf 1 is therefore assumed to extend to the base of the Cyprina Clay at 232 cm. The two lowest samples, at 229 and 220 cm, contain nearly monospecific assemblages of short-processed cysts of *Gonyaulax baltica* (Fig. 9a–d, and as *Spiniferites* spp. undifferentiated in Fig. 4) accompanied by rare specimens of *Operculodinium centrocarpum*. *Gonyaulax baltica* has been shown in laboratory culturing experiments to grow within a wide range of salinities (between 5 and 55 psu for the strain analysed by Ellegaard, Lewis & Harding, 2002). Cysts of *Gonyaulax baltica* have been reported from modern sediments of the Baltic as *Spiniferites bulloideus* (N. Gundersen, unpub. Cand. Scient. Dissertation, Univ. Oslo, 1988), *Spiniferites* cf. *bulloideus* (Matthiessen & Brenner, 1996), *Spiniferites* sp. (Dale, 1988) and as *Spiniferites* spp. (Ellegaard, 2000). Dale (1996) examined the modern distribution of these cysts in the Baltic Sea, and reported a tolerance of salinities down to 0.03–0.5 psu. Moreover, he noted that below salinities of 3 psu, cysts of *Gonyaulax baltica* and morphotypes of *O. centrocarpum* were the only marine dinoflagellate cysts present. Accordingly, the lowest two samples of zone RKDf 1, at 229 and 220 cm, are considered to represent salinities greater than 0.03–0.5 psu and less than about 3 psu.

Kristensen *et al*. (2000) reported the lowest occurrence of benthic foraminifers at 223 cm (6 cm above that of dinoflagellate cysts) represented by a monospecific assemblage of *Elphidium albiumbilicatum*. This species appears not to tolerate salinities below about 3.5 psu (Rottgardt, 1952), accounting for its appearance later than the dinoflagellates. Furthermore, the dinoflagellates will have proliferated immediately upon arrival with the surface water ingression, whereas the benthic foraminifera will have required conditions to stabilize before colonizing the bottom substrate.

An assemblage at 208 cm contains significant peaks of *Operculodinium centrocarpum*–short processes and *Operculodinium centrocarpum* var. *cezare,* morphotypes that are known to indicate low salinities (Dale, 1988, 1996; de Vernal, Goyette & Rodrigues, 1989; Matthiessen & Brenner, 1996; Nehring, 1997; Ellegaard, 2000; Brenner, 2001*b*; Brenner & Meemken, 2002). The average process length rarely exceeds 3 μm for any of the *Operculodinium centrocarpum* morphotypes in this sample (Figs 4, 5). The assemblage also contains the earliest significant numbers of *Lingulodinium machaerophorum* (7 %), these specimens also having reduced process lengths (less than 6 μm long; Fig. 5). Of four specimens of *Spiniferites bentorii* counted in this sample, three have processes that are reduced in length and development. Based on the distribution of morphotypes in the Baltic Sea today, a dominance of short-processed over long-processed forms of *O. centrocarpum* should indicate salinities of less than 7 psu, whereas the presence of *L. machaerophorum* should indicate salinities of 7 psu or more (Dale, 1996). The assemblage at 208 cm, where

short-processed forms of *O. centrocarpum* dominate along with subordinate *L. machaerophorum*, should therefore represent salinities close to 7 psu. Stunted processes in the specimens of *L. machaerophorum* and *S. bentorii* imply that these euryhaline species are close to the limits of their salinity tolerance.

The assemblage at 208 cm coincides with an abrupt increase in the omnivorous benthic foraminifer *Ammonia beccarii*. This indicates an environmental change, presumably triggered by an increase in salinity or nutrients, that affected both planktonic and benthic taxa.

The absence of *Pyxidinopsis psilata* from zone RKDf 1 (and higher in the sequence) is worthy of comment. This species is considered characteristic of low-salinity (3–10 psu) environments today in the Baltic Sea, sometimes exceeding 75 % of assemblages in the central Baltic where salinities are around 7 psu (Dale, 1996). This species was also locally abundant in the Baltic Sea during the early Holocene (Brenner, 2001*a*, *b*) and similarly characterized low-salinity phases of the Black Sea during late Quaternary time. Apparently, *Pyxidinopsis psilata* requires very specific and as yet unknown environmental conditions to thrive (Brenner, 2001*a*).

The highest sample of zone RKDf 1 at 190 cm is again dominated by cysts of *Gonyaulax baltica*, but *Lingulodinium machaerophorum*, at 15 %, suggests that salinities had risen to about 15 psu or more (Brenner, 2001*b*). This progressive increase in salinity is supported by an increase in process length both for *L. machaerophorum* and *O. centrocarpum* (Fig. 5), and by a rise in the number of dinoflagellate cyst taxa from 6 taxa at 208 cm to 14 taxa at 190 cm.

Surface water palaeotemperatures for zone RKDf 1 can only be ascertained from 208 cm and upwards, where the presence of the tropical to temperate species *Lingulodinium machaerophorum* indicates warm summers. The thermophilic species *Tectatodinium pellitum* (Fig. 9i, j) and *Tuberculodinium vancampoae* (Fig. 9k), which are Lusitanian–Mediterranean elements today, make their first appearance at 190 cm and attest to summer temperatures greater than present at least by the end of zone RKDf 1.

Benthic foraminifera for the interval represented by zone RKDf 1 comprise a low diversity assemblage, reflecting shallow, brackish conditions (Kristensen *et al*. 2000). A progressive rise in the concentration of benthic foraminifera through this interval (Kristensen *et al*. 2000) follows a similar rise within dinoflagellate cyst concentrations (Fig. 3) and may reflect progressively rising salinities.

10.c. RKDf 2 (187–58.5 cm) *Lingulodinium machaerophorum* Assemblage Biozone, *c*. 750–1900 years into Eemian

An abrupt rise in cyst concentration (Fig. 3) and diversity (Fig. 4) beginning with the lowest sample of this zone, at 184 cm, is interpreted as a sharp rise in salinity. Comparison with the Kiel Bight and Kattegat of the present Baltic Sea, where cyst assemblages of comparable diversity have been reported (Nehring, 1994, 1997; Ellegaard, Christensen & Moestrup, 1994; Persson, Godhe & Karlson, 2000), suggests salinities in excess of about 15 psu at the beginning of zone RKDf 2. Process length in *O. centrocarpum* also increases significantly across the RKDf 1–2 boundary, implying a rapid rise in salinity, although this feature is not discernible in *L. machaerophorum* (Fig. 5). In general, however, increasing process length for both *L. machaerophorum* and *O. centrocarpum* (Fig. 5) implies a small but progressive rise in salinity through most of zone RKDf 2, a trend reflected also in the steady appearance of new taxa particularly from the base of the zone to 130 cm (Table 1).

Benthic foraminifera also reveal evidence of a sharp increase in salinity at around 187 cm (the base of zone RKFO 4 of Kristensen *et al*. 2000), and the appearance of a *Haynesina orbiculare* association together with *Elphidium incertum* at this time indicates a salinity above 22 psu (Kristensen *et al*. 2000). Evidence from molluscs from the lower part of the Cyprina Clay exposed at various southwestern Baltic sites points to an initial brackish phase followed by salinities around 25 to 30 psu (Funder, Demidov & Yelovicheva, 2002).

The dinoflagellate cysts provide a strong temperature signal in zone RKDf 2. The persistent presence of *Tectatodinium pellitum* (Fig. 9i–j) and *Tuberculodinium vancampoae* (Fig. 9k) throughout this zone indicates warmer summer sea-surface temperatures than today. Neither species is found in the Baltic Sea or North Sea today. A single report of *Pyrophacus steinii* (the vegetative stage of *Tuberculodinium vancampoae*) from the southeastern North Sea (Nehring, 1995, table 2) is refuted by M. Elbrächter (pers. comm. 2000). In zone RKDf 2, *T. vancampoae* reaches peak values of 11.8 % at 66 cm. Based on its global distribution, this tropical to warm-temperate coastal species presently has abundances above 3 % mostly where summer sea-surface temperatures are between 26° and 28 °C, and abundances above 10 % only where temperatures reach 27 °C (Marret & Zonneveld, 2003). The abundance of this species therefore suggests that summer sea-surface temperatures for the upper part of zone RKDf 2 were at least 5 °C higher than today in the southwest Baltic Sea. In this zone and throughout the Ristinge Klint section, cool-water species such as *Bitectatodinium tepikiense* (Fig. 7e, f) and *Spiniferites frigidus* occur only as isolated specimens. The paucity of cold-water species is highly significant, as it means that not only did temperatures reach a brief high peak in summer but waters were warm during the spring bloom, too, implying mild winter temperatures.

Subzone RKDf 2b (70.5–58.5 cm) is characterized by an absence of invertebrate eggs and the cysts of heterotrophic dinoflagellates, which are well

represented throughout the subjacent subzone RKDf 2a (187–70.5 cm). Moreover, heterotrophic dinoflagellate cysts appear only rarely in the superjacent zone RKDf 3 and their pale and delicate state of preservation indicates partial oxidation. These microfossil groups, and also invertebrate mouthparts/appendages which disappear above 60 cm, are well known to be particularly susceptible to oxidation. Their virtual disappearance from about 70.5 cm therefore results from partial oxidation of the sediments. This oxidation may have been caused by subsequent diagenesis or weathering of the deposits at Ristinge Klint, but alternatively signifies the presence of well-oxygenated bottom currents at the time of deposition (see below).

From 66 cm to the top of the section, the primarily arctic–subarctic benthic foraminifera *Buccella frigida* and *Haynesina nivea* and the benthic ostracode *Robertsonites tuberculatus* all reach maximum frequencies (Kristensen *et al*. 2000). Kristensen *et al*. (2000) surmised that these species reflect either a general cooling of the water column, or more likely that continued sea-level rise had caused cold and saline bottom waters (below the pycnocline) to move into the site of deposition. The presence of thermophilic dinoflagellate cysts throughout subzone RKDf 2b and to the top of the section, and a continuing paucity of cool-water species, demonstrates that the water column had indeed become thermally stratified, with the surface waters remaining warm. The intrusion of cold bottom waters into the site at this time may also account for the disappearance of oxidation-susceptible heterotrophic dinoflagellate cysts and other palynomorphs. The suggestion that these bottom waters were well oxygenated is supported by evidence from mollusc faunas at Ristinge Klint, which are poor in anoxia-tolerant species compared with many other sites in the Baltic (Funder & Balic-Zunic, 2006).

Although the autecology of *Achomosphaera andalousiensis* (Fig. 7g–i) is not well known, its first appearance at the base of subzone RKDf 2b is perhaps a response to increasing salinity.

10.d. RKDf 3 (58.5–3 cm) *Ataxiodinium choane* Assemblage Biozone, *c*. 1900– < 3000 years into Eemian

Zone RKDf 3 represents the highest part of the Cyprina Clay at Ristinge Klint. The persistent occurrence of the tropical to warm-temperate species *Tuberculodinium vancampoae* (2.3–8.4 %) and *Tectatodinium pellitum* and paucity of cool-water species attest to surface waters that continued to be significantly warmer than today. The occurrence of *Capisocysta lata* (Fig. 9l–p), a tropical to warm-temperate neritic species (Head, 1998), at the upper part of this zone seems significant, although it is not clear whether increasing temperature, salinity or other environmental factors are the cause. Process length in *Lingulodinium machaerophorum* is more or less constant throughout this zone, although a slight decrease in process length for *Operculodinium centrocarpum* (Fig. 5) implies a small lowering in salinity. However, other lines of evidence show somewhat increasing salinity or marine influence through zone RKDf 3. The first appearance of *Ataxiodinium choane* (Figs 6p–s, 7a–d) at the base of this zone suggests increasing salinity, as this species is not generally recorded from sites with reduced salinities and has a wide tolerance of temperatures (Marret & Zonneveld, 2003). A steady decline in *Lingulodinium machaerophorum*, from 51 % at the base of the zone to 19 % at the top, while *Operculodinium centrocarpum* and *Spiniferites bentorii* show a slight increase, seems to indicate increasing salinity and/or hydrographic stability. A comparable decline in *L. machaerophorum*, which is a euryhaline and typically estuarine species, has been similarly interpreted for dinoflagellate cysts from the Eemian of the southeastern Baltic Sea (Head *et al*. 2005, p. 24). *Operculodinium centrocarpum* is a cosmopolitan species whose present distribution closely matches that of the Gulf Stream and North Atlantic Current (Rochon *et al*. 1999, p. 13), and its rising frequency in this zone appears to reflect an increased inflow of North Sea waters into the Baltic Sea at this time. A decrease in the concentration of bisaccate pollen appears also to signal increasing distance from shore through zone RKDf 3.

Despite warm surface waters, the bottom waters remained cold, judging from the benthic foraminifera (Kristensen *et al*. 2000), and the water column was thermally stratified at least seasonally throughout zone RKDf 3. Almost normal marine conditions are observed for the benthic foraminifera, but no oceanic dinoflagellate cysts (especially of the genus *Impagidinium*) have been recorded from Ristinge Klint. Hence, although summer sea-surface salinities were high and probably increasing through zone RKDf 3, conditions were not fully oceanic. Moreover, process length in *O. centrocarpum* is generally between 5 and 8 μm in zone RKDf 3, whereas modern specimens from the southeastern North Sea, where the summer sea surface salinity is about 30.0–34.5 psu, have processes mainly around 9–13 μm in length (Nehring, 1997, fig. 43).

11. Ristinge Klint and other Baltic dinoflagellate cyst floras compared

The only other Eemian localities in the Baltic region where dinoflagellate cysts have been studied in any detail are at Mommark in Denmark (M. J. Head, unpub. data), the Licze borehole in Poland (Head *et al*. 2005) and Mertuanoja in Ostrobothnia (Eriksson, Grönlund & Uutela, 1999; Fig. 2). Immediately beyond the Baltic, Eemian dinoflagellate cysts have been described from the Amsterdam-Terminal borehole in the Netherlands (van Leeuwen *et al*. 2000) and from the White Sea

region of northwestern Russia (Grøsfjeld *et al*. 2006). The Ristinge Klint flora is almost identical with that of Mommark, which is situated only about 40 km to the WNW of Ristinge Klint (Fig. 1). The Licze borehole in Poland is also very similar, the only significant difference being the presence of *Stelladinium* spp. (Figs 11m–q, 12a–e) and *Achomosphaera andalousiensis* (Fig. 7g–i) at Ristinge Klint. Perhaps conditions were somewhat more restricted at Licze. The Amsterdam-Terminal borehole flora is not fully documented but, as with Ristinge Klint, Mommark and Licze, contains the characteristic thermophilic species *Tuberculodinium vancampoae*. The flora at Mertuanoja is notably less diverse than these other sites, and likely reflects less saline and perhaps cooler surface-water conditions (Head *et al*. 2005). In particular, the tropical–subtropical *Polysphaeridium zoharyi* var. *ktana* as reported by Eriksson, Grönlund & Uutela (1999, fig. 7E) is a misidentified short-processed (low salinity) morphotype of the cosmopolitan species *Operculodinium centrocarpum*. The flora from the White Sea region (Grøsfjeld *et al*. 2006) differs from any known Baltic flora in reflecting much lower temperatures and including significant numbers of the cold-water species *Islandinium minutum*.

Marine interglacial deposits from the Skagen 3 borehole, located at the northeast tip of Jutland (Fig. 1), have been reported as late Eemian (Glaister & Gibbard, 1998), tentatively late Eemian (C. G. Glaister, unpub. Ph.D. thesis, Univ. Cambridge, 2000), questionably Eemian (Turner, 2000), or possibly an older interglacial (Sejrup & Knudsen, 1999). The dinoflagellate cysts have been studied by A. Rochon (unpub. Ph.D. thesis, Univ. du Québec à Montréal, 1997) and include *L. machaerophorum* (below 5 %), *Bitectatodinium tepikiense* (10–15 %) and *Islandinium minutum* (up to 5 %). This is unlike any assemblage reported from the Eemian of the Baltic (including Mommark, where a complete record of the Eemian exists) or the Amsterdam-Terminal borehole in the Netherlands, and indicates cooler conditions. The Skagen 3 deposits therefore are either not of Eemian age, or the assemblage is the result of a different hydrographic setting at this more open-marine site.

12. Summary and conclusions

This is the first detailed record of dinoflagellate cysts from the Eemian of the southwestern Baltic, documenting almost 3000 years of early Eemian time as determined by the recalibration of a previously published record of the pollen flora (Kristensen *et al*. 2000). During the Eemian, a distinctive dinoflagellate cyst flora with strong Mediterranean/Lusitanian affinities occupied the southern North Sea and Belt Sea, and extended eastwards along the southern margin of the Baltic Sea at least as far as Poland (Head *et al*. 2005). This may not be surprising, given that the Eemian represents the warmest Quaternary interglacial known for the Baltic region (Donner, 1995), and highlights the potential utility for dinoflagellate cyst studies to distinguish Eemian marine deposits from earlier interglacial deposits in the Baltic region. This would be helpful particularly in cases where pollen assemblages are rendered unreliable by marine taphonomic processes. No published studies of dinoflagellate cysts are known for these earlier interglacials, but such studies are essential to test the stratigraphic utility of Quaternary dinoflagellate cysts in the Baltic region.

The oldest Eemian deposits at Ristinge Klint are the ‘Shiny Clay’. Palynology indicates a freshwater origin for this unit, and the overlying Freshwater Sand, although barren of palynomorphs, is lacustrine based on other evidence. The superjacent Cyprina Clay marks the onset marine of marine conditions, with a low-salinity marine dinoflagellate cyst assemblage occurring just above the base. The marine ingression at Ristinge Klint is confirmed as having occurred 300 years after the Eemian onset, that is, within the *Quercus* rise, and similar in timing to the ingression at Mommark (Kristensen & Knudsen, 2006). This contrasts with sites to the east where marine influence is established as early as late Saalian at Plasumi in Latvia and earliest Eemian at Prangli in Estonia (Funder, Demidov & Yelovicheva, 2002), and within the first 300 years at Licze in Poland (Head *et al*. 2005) (Fig. 2). Evidently a North Sea connection with these eastern sites existed for several hundred years before the marine inundation of Ristinge Klint and Mommark. The late arrival of marine waters at Ristinge Klint and Mommark is explained by higher site elevations (Head *et al*. 2005).

During an interval from 300 years to 750 years after the beginning of Eemian time, representing the lowest 45 cm of the Cyprina Clay, salinities rose progressively from less than 3 psu at the base to about 15 psu or more at the top. Process lengths of *Operculodinium centrocarpum* and *Lingulodinium machaerophorum* also increase progressively during this time, attesting to the usefulness of this feature for assessing salinity changes in brackish palaeoenvironments. Dinoflagellate cyst production was low during this brackish interval.

At 750 years (*c*. 650 years at the time scale of Kristensen *et al*. 2000) after the Eemian onset, an abrupt rise in sea-surface salinity is inferred both from the dinoflagellate cyst and benthic foraminiferal records. This event has been attributed to an opening of the Danish portal (Kristensen *et al*. 2000), and seems also to correspond to a similar sharp rise in salinity at Licze in Poland (Head *et al*. 2005). Whether this is indeed a Baltic-wide event, or represents local hydrographic changes within perhaps restricted depositional basins, will require additional detailed studies at other localities.

There seems to have been a small but progressive rise in salinity from about 750 to 1900 years. Indeed, from about 750 years to the end of the record at Ristinge Klint, the dinoflagellate cysts reflect considerably higher salinities than today. Surface-water temperatures were also warmer than today from about 750 years onwards, and before this time were presumably warmer than today, but the low salinity will have excluded key thermophilic species.

At about 1900 years after the start of the Eemian, and continuing to the top of the section (almost 3000 years after the start of the Eemian), high values of the tropical–warm-temperate species *Tuberculodinium vancampoae* suggest summer sea-surface temperatures of between 26° and 28 °C which is more than 5 °C higher than today. Moreover, the paucity of cool-water species throughout the Ristinge Klint record suggests mild spring temperatures and implicitly mild winter temperatures. This agrees with evidence from molluscs of the Belt Sea area and Poland which indicates winter sea-surface temperatures of *c*. 9 °C, which is 6 °C warmer than at present (Funder, Demidov & Yelovicheva, 2002).

Also from about 1900 years after the start of the Eemian, cold bottom waters became established at Ristinge Klint (Kristensen *et al*. 2000), indicating thermal stratification of the water column, at least during summer. The water column remained thermally stratified throughout the remaining record. Increasing water depth has been suggested as a possible explanation (Kristensen *et al*. 2000).

On balance, evidence from dinoflagellate cysts points to somewhat increasing salinity and more open-marine conditions during the last thousand years at Ristinge Klint, although fully oceanic salinities were never attained. Dinoflagellate cyst assemblages are broadly consistent with interpretations, based on molluscs (Funder, Demidov & Yelovicheva, 2002), that salinities attained between 25 and 30 psu in the Belt Sea.

The pollen dated sea-level curve of Zagwijn (1983, 1996) for the Eemian from the southern North Sea indicates a rising sea level until about 3500 years into the interglacial. Evidence from Ristinge Klint, which records almost the first 3000 years of Eemian time, supports a rising sea level throughout this time.

The warm interval recorded at Ristinge Klint can be assessed against northwest European terrestrial temperatures reconstructed from palaeobotanical and coleopteran evidence. Terrestrial summer temperatures reached a maximum between *c*. 300 and 1900 years before the Eemian onset (Zagwijn, 1996; Aalbersberg & Litt, 1998). However, sea-surface temperatures at Ristinge Klint remained high for at least another 1000 years despite declining summer temperatures on land, and this would have required the inflow of particularly warm North Sea water during this time. An English Channel transporting more Atlantic water into the southern North Sea than during the Holocene (Funder, Demidov & Yelovicheva, 2002), and the influence of a stronger North Atlantic Current at this time (Weaver & Hughes, 1994; Knudsen, Seidenkrantz & Kristensen, 2002; Cape Last Interglacial Project Members, 2006), could both explain this prolonged heat flux into the Baltic Sea.

As with Licze in Poland (Head *et al.* 2005), there is no evidence from the dinoflagellate cyst record at Ristinge Klint for the influence of Arctic watermasses, at least within the surface waters. This is consistent with the view that the White Sea–Baltic seaway was not a major corridor for water exchange (Funder, Demidov & Yelovicheva, 2002).

Acknowledgements. The present study is a contribution to the European-Community funded BALTEEM project. It was undertaken at the suggestion of P. L. Gibbard (BALTEEM Leader, Cambridge) and has benefited from his enthusiastic support. Samples were kindly supplied by P. Kristensen (Aarhus). Enlightening discussions also with B. Dale (Oslo), P. Kristensen and K.-L. Knudsen (both Aarhus) are gratefully acknowledged, as is laboratory assistance from S. Boreham (Cambridge) and W. Gosling (now Open University). Thoughtful reviews of the manuscript by R. Harland (Bingham, UK), James B. Riding (Keyworth, UK) and an anonymous reviewer are sincerely appreciated. This study was initiated during a Visiting Fellowship at Wolfson College, Cambridge.

References

AALBERSBERG, G. & LITT, T. 1998. Multiproxy climate reconstructions for the Eemian and Early Weichselian. *Journal of Quaternary Science* **13**, 367–90.

ANDERSEN, S. T. 1961. Vegetation and its environment in Denmark in the Early Weichselian Glacial (Last Glacial). *Danmarks Geologiske Undersøgelse, II Række* **75**, 1–175.

ANDERSEN, S. T. 1975. The Eemian freshwater deposit at Egernsund, South Jylland, and the Eemian landscape development in Denmark. *Danmarks Geologiske Undersøgelse Årbog 1974*, 49–70.

BALECH, E. 1988. Los dinoflagelados del Atlántico Sudoccidental. *Publicaciónes Especiales Instituto Español de Oceanografía* **1**, 1–310.

BEETS, D. J., BEETS, C. J. & CLEVERINGA, P. 2006. Age and climate of the late Saalian and early Eemian in the type-area, Amsterdam basin, The Netherlands. *Quaternary Science Reviews* **25**, 876–85.

BRADFORD, M. R. 1975. New dinoflagellate cyst genera from the recent sediments of the Persian Gulf. *Canadian Journal of Botany* **53**, 3064–74.

BRENNER, W. W. 2001*a*. Distribution of organic walled microfossils within single lamina from the Gotland Basin, and their environmental evidence. *Baltica* **14** (2001), 34–9.

BRENNER, W. W. 2001*b*. Organic-walled microfossils from the central Baltic Sea, indicators of environmental change and base for ecostratigraphic correlation. *Baltica* **14** (2001), 40–51.

BRENNER, W. & MEEMKEN, H.-J. 2002. Öko- und chronostratigraphische Korrelierung der Zentralen Ostsee mit

der Kieler Bucht anhand organisch-wandiger Mikrofossilien. *Meyniana* **54**, 17–40.

BÜTSCHLI, O. 1885. Erster Band. Protozoa. In *Dr. H.G. Bronn's Klassen und Ordnungen des Thier-Reiches, wissenschaftlich dargestellt in Wort und Bild*, pp. 865–1088. Leipzig and Heidelberg: C.F. Winter'sche Verlagshandlung.

CAPE LAST INTERGLACIAL PROJECT MEMBERS. 2006. Last Interglacial arctic warmth confirms polar amplification of climate change. *Quaternary Scince Reviews* **25**, 1383–1400.

CHRISTENSEN, T., KOCH, C. & THOMSEN, H. A. 1985. *Distribution of Algae in Danish Salt and Brackish Waters*. Institut for Sporeplanter, University of Copenhagen.

CLIMAP PROJECT MEMBERS. 1984. The Last Interglacial ocean. *Quaternary Research* **21**, 123–4.

DALE, B. 1983. Dinoflagellate resting cysts: "benthic plankton". In *Survival strategies of the algae* (ed. G. A. Fryxell), pp. 69–136. Cambridge, UK: Cambridge University Press.

DALE, B. 1988. Low salinity dinoflagellate cyst assemblages from Recent sediments of the Baltic region. *Seventh International Palynological Congress, Brisbane, Abstracts*, p. 33.

DALE, B. 1996. Dinoflagellate cyst ecology: modeling and geological applications. In *Palynology: Principles and Applications. Volume 3* (eds J. Jansonius & D. C. McGregor), pp. 1249–75. Dallas, Texas: American Association of Stratigraphic Palynologists Foundation.

DEFLANDRE, G. & COOKSON, I. C. 1955. Fossil microplankton from Australian Late Mesozoic and Tertiary sediments. *Australian Journal of Marine and Freshwater Research* **6**(2), 242–313.

DE VERNAL, A., GOYETTE, C. & RODRIGUES, C. G. 1989. Contribution palynostratigraphique (dinokystes, pollen et spores) à la connaissance de la mer de Champlain: coupe de Saint-Césaire, Québec. *Canadian Journal of Earth Sciences* **26**, 2450–64.

DE VERNAL, A., HENRY, M., MATTHIESSEN, J., MUDIE, P. J., ROCHON, A., BOESSENKOOL, K. P., EYNAUD, F., GRØSFJELD, K., GUIOT, J., HAMEL, D., HARLAND, R., HEAD, M. J., KUNZ-PIRRUNG, M., LEVAC, E., LOUCHEUR, V., PEYRON, O., POSPELOVA, V., RADI, T., TURON, J.-L. & VORONINA, E. 2001. Dinoflagellate cyst assemblages as tracers of sea-surface conditions in the northern North Atlantic, Arctic and sub-Arctic seas: the new 'n = 677' data base and its application for quantitative palaeoceanographic reconstruction. *Journal of Quaternary Science* **16**, 681–98.

DONNER, J. 1995. *The Quaternary history of Scandinavia*. Cambridge, UK: Cambridge University Press, 200 pp.

EDLER, L., HÄLFORS, G. & NIEMI, Å. 1984. A preliminary check-list of the phytoplankton of the Baltic Sea. *Acta Botanica Fennica* **128**, 1–26.

ELLEGAARD, M. 2000. Variations in dinoflagellate cyst morphology under conditions of changing salinity during the last 2000 years in the Limfjord, Denmark. *Review of Palaeobotany and Palynology* **109**, 65–81.

ELLEGAARD, M., CHRISTENSEN, N. F. & MOESTRUP, Ø. 1994. Dinoflagellate cysts from Recent Danish marine sediments. *European Journal of Phycology* **29**, 183–94.

ELLEGAARD, M., LEWIS, J. & HARDING, I. 2002. Cyst–theca relationship, life cycle, and effects of temperature and salinity on the cyst morphology of *Gonyaulax baltica* sp. nov. (Dinophyceae) from the Baltic Sea area. *Journal of Phycology* **38**, 775–89.

ERIKSSON, B., GRÖNLUND, T. & UUTELA, A. 1999. Biostratigraphy of Eemian sediments at Mertuanoja, Pohjanmaa (Ostrobothnia), western Finland. *Boreas* **28**, 274–91.

FENSOME, R. A., TAYLOR, F. J. R., NORRIS, G., SARJEANT, W. A. S., WHARTON, D. I. & WILLIAMS, G. L. 1993. *A classification of living and fossil dinoflagellates*. Micropaleontology Special Publication Number 7, i–viii, 1–351.

FENSOME, R. A. & WILLIAMS, G. L. 2004. The Lentin & Williams index of fossil dinoflagellates 2004 edition. *American Association of Stratigraphic Palynologists Contributions Series* **42**, 1–909.

FIELD, M. H., HUNTLEY, B. & MÜLLER, H. 1994. Eemian climate fluctuations observed in a European pollen record. *Nature* **371**, 779–83.

FUNDER, S. & BALIC-ZUNIC, T. 2006. Hypoxia in the Eemian: mollusk faunas and sediment mineralogy from Cyprina Clay in the south Baltic region. *Boreas* **35**, 367–77.

FUNDER, S., DEMIDOV, I. & YELOVICHEVA, Y. 2002. Hydrography and mollusc faunas of the Baltic and White Sea–North Sea seaway in the Eemian. *Palaeogeography, Palaeoclimatology, Palaeoecology* **184**, 275–304.

GIBBARD, P. L. & GLAISTER, C. 2006. Pollen stratigraphy of the Late Pleistocene sediments at Mommark, Als, South Denmark. *Boreas* **35**, 332–48.

GLAISTER, C. G. & GIBBARD, P. L. 1998. Pollen stratigraphy of Late Pleistocene marine sediments at Nørre Lyngby and Skagen, North Denmark. *Quaternary Science Reviews* **17**, 839–54.

GREUTER, W., MCNEILL, J., BARRIE, F. R., BURDET, H. M., DEMOULIN, V., FILGUEIRAS, T. S., NICOLSON, D. H., SILVA, P. C., SKOG, J. E., TREHANE, P., TURLAND, N. J. & HAWKSWORTH, D. L. 2000. International Code of Botanical Nomenclature (Saint Louis Code). *Regnum Vegetabile* **138**, i–xviii, 1–474.

GRØSFJELD, K., FUNDER, S., SEIDENKRANTZ, M.-S. & GLAISTER, C. 2006. Last Interglacial marine environments in the White Sea region, northwestern Russia. *Boreas* **35**, 493–520.

GRØSFJELD, K. & HARLAND, R. 2001. Distribution of modern dinoflagellate cysts from inshore areas along the coast of southern Norway. *Journal of Quaternary Science* **16**, 651–9.

HAECKEL, E. 1894. *Systematische Phylogenie. Entwurf eines natürlichen Systems der Organismen auf Grund ihrer Stammegeschichte, I. Systematische Phylogenie der Protisten und Pflanzen*, pp. i–xv, 1–400. Berlin: Reimer.

HAILA, H., MIETTINEN, A. & ERONEN, M. 2006. Diatom succession of a dislocated Eemian sediment sequence at Mommark, South Denmark. *Boreas* **35**, 378–84.

HANSEN, G. & LARSEN, J. 1992. Dinoflagellater i danske farvande. In *Plankton i de indre danske farvande* (ed. H. A. Thomsen), pp. 45–155. Copenhagen: Havforskning fra Miljøstyrelsen, Nr. 11.

HARLAND, R. 1982. A review of Recent and Quaternary organic-walled dinoflagellate cysts of the genus *Protoperidinium*. *Palaeontology* **25**, 369–97.

HEAD, M. J. 1996*a*. Modern dinoflagellate cysts and their biological affinities. In *Palynology: principles and applications. Volume 3* (eds J. Jansonius & D. C. McGregor), pp. 1197–1248. Dallas, Texas: American Association of Stratigraphic Palynologists Foundation.

HEAD, M. J. 1996*b*. Late Cenozoic dinoflagellates from the Royal Society borehole at Ludham, Norfolk, eastern England. *Journal of Paleontology* **70**, 543–70.

HEAD, M. J. 1998. New goniodomacean dinoflagellates with a compound hypotractal archeopyle from the late Cenozoic: *Capisocysta* Warny and Wrenn, emend. *Journal of Paleontology* **72**, 797–809.

HEAD, M. J. 2003. *Echinidinium zonneveldiae* sp. nov., a dinoflagellate cyst from the Late Pleistocene of the Baltic Sea, northern Europe. *Journal of Micropalaeontology* **21**, 169–73 (imprinted, 2002).

HEAD, M. J., HARLAND, R. & MATTHIESSEN, J. 2001. Cold marine indicators of the late Quaternary: the new dinoflagellate cyst genus *Islandinium* and related morphotypes. *Journal of Quaternary Science* **16**, 621–36.

HEAD, M. J., SEIDENKRANTZ, M.-S., JANCZYK-KOPIKOWA, Z., MARKS, L. & GIBBARD, P. L. 2005. Last Interglacial (Eemian) hydrographic conditions in the southeastern Baltic Sea, NE Europe, based on dinoflagellate cysts. *Quaternary International* **130**, 3–30.

HEIMDAL, B. R., HASLE, G. R. & THRONDSEN, J. 1973. An annotated check-list of plankton algae from the Oslofjord, Norway (1951–1972). *Norwegian Journal of Botany* **20**, 13–19.

JOHNSTRUP, F. 1882. *Nogle Iagttagelser over Glacialphaenomenerne af Cyprina-leret i Danmark*. 74 pp. København: Univ. Program Kongens Födselsdag 1881.

KNUDSEN, K. L. 1985. Foraminiferal faunas in Eemian deposits of the Oldenbüttel area near the Kiel Canal, Germany. *Geologisches Jahrbuch, A* **86**, 27–47.

KNUDSEN, K.-L., SEIDENKRANTZ, M.-S. & KRISTENSEN, P. 2002. Last interglacial and early glacial circulation in the northern North Atlantic. *Quaternary Research* **58**, 22–6.

KOSACK, B. & LANGE, W. 1985. Das Eem-Vorkommen von Offenbüttel/Schnittlohe und die Ausbreitung des Eem-Meeres zwischen Nord- und Ostsee. *Geologisches Jahrbuch, A* **86**, 3–17.

KRISTENSEN, P., GIBBARD, P., KNUDSEN, K. L. & EHLERS, J. 2000. Last interglacial stratigraphy at Ristinge Klint, South Denmark. *Boreas* **29**, 103–16.

KRISTENSEN, P. H. & KNUDSEN, K. L. 2006. Palaeoenvironments of a complete Eemian sequence at Mommark, South Denmark: foraminifera, ostracods and stable isotopes. *Boreas* **35**, 349–66.

LINDEMANN, E. 1928. Abteilung Peridineae (Dinoflagellatae). In *Die Natürlichen Pflanzenfamilien nebst ihren Gattungen und wichtigeren Arten insbesondere den Nutzpflanzen* (eds A. Engler & K. Prantl), pp. 3–104. Zweite stark vermehrte und verbesserte Auflage herausgegeben von A. Engler. 2 Band. Leipzig: Wilhelm Engelmann.

MADSEN, V., NORDMANN, V. & HARTZ, N. 1908. Eem-Zonerne. Studier over Cyprinaleret og andre Eem-Aflejringer i Danmark, Nord-Tyskland og Holland. *Danmarks Geologiske Undersøgelse II* **17**, 1–302.

MANTELL, G. A. 1850. *A Pictorial Atlas of Fossil Remains, Consisting of Coloured Illustrations Selected from Parkinson's "Organic Remains of a Former World", and Artis's "Antediluvian Phytology"*, pp. xii+207, 74 pl. London, UK: Henry G. Bohn.

MARRET, F. & ZONNEVELD, K. A. F. 2003. Atlas of modern organic-walled dinoflagellate cyst distribution. *Review of Palaeobotany and Palynology* **125**, 1–200.

MATSUOKA, K., MCMINN, A. & WRENN, J. H. 1997. Restudy of the holotype of *Operculodinium centrocarpum* (Deflandre & Cookson) Wall (Dinophyceae) from the Miocene of Australia, and the taxonomy of related species. *Palynology* **21**, 19–33.

MATTHIESSEN, J. & BRENNER, W. 1996. Chlorococcalalgen und Dinoflagellaten-Zysten in rezenten Sedimenten des Greifswalder Boddens (südliche Ostsee). *Senckenbergiana Maritima* **27**, 33–48.

MÜLLER, H. 1974. Pollenanalytische Untersuchungen und Jahresschichtenzählungen an der eem-zeitlichen Kieselgur von Bispingen/Luhe. *Geologisches Jahrbuch A* **21**, 149–69.

NEHRING, S. 1994. Spatial distribution of dinoflagellate resting cysts in Recent sediments of Kiel Bight, Germany (Baltic Sea). *Ophelia* **39**, 137–58.

NEHRING, S. 1995. Dinoflagellate resting cysts as factors in phytoplankton ecology of the North Sea. *Helgoländer Meeresuntersuchungen* **49**, 375–92.

NEHRING, S. 1997. Dinoflagellate resting cysts from Recent German coastal sediments. *Botanica Marina* **40**, 307–24.

OTTO-BLIESNER, B. L., MARSHA, S. J., OVERPECK, J. T., MILLER, G. H. & HU, A. X. 2006. Simulating arctic climate warmth and icefield retreat in the last interglaciation. *Science* **311**, 1751–3.

OVERPECK, J. T., OTTO-BLIESNER, B. L., MILLER, G. H., MUHS, D. R., ALLEY, R. B. & KIEHL, J. T. 2006. Paleoclimatic evidence for future ice-sheet instability and rapid sea-level rise. *Science* **311**, 1747–50.

PANKOW, H. 1990. *Ostsee-Algenflora*. Jena: Fischer, 648 pp.

PASCHER, A. 1914. Über Flagellaten und Algen. *Berichte der Deutschen Botanischen Gesellshaft* **36**, 136–60.

PERSSON, A., GODHE, A. & KARLSON, B. 2000. Dinoflagellate cysts in recent sediments from the west coast of Sweden. *Botanica Marina* **43**, 69–79.

RAUKAS, A. 1991. Eemian interglacial record in the northwestern European part of the Soviet Union. *Quaternary International* **10–12**, 183–9.

REID, P. C. 1974. Gonyaulacacean dinoflagellate cysts from the British Isles. *Nova Hedwigia* **25**, 579–637.

ROCHON, A., DE VERNAL, A., TURON, J.-L., MATTHIESSEN, J. & HEAD, M. J. 1999. Distribution of recent dinoflagellate cysts in surface sediments from the North Atlantic Ocean and adjacent seas in relation to sea-surface parameters. *American Association of Stratigraphic Palynologists, Contributions Series* **35**, 1–146.

ROTTGARDT, D. 1952. Mikropalaöntologische wichtige Bestandteile rezenter brakischer Sedimente an den Küsten Schleswig-Holsteins. *Meyniana* **1**, 169–228.

SÁNCHEZ-GOÑI, M. F., EYNAUD, F., TURON, J.-L. & SHACKLETON, N. J. 1999. High-resolution palynological record off the Iberian margin: direct land/sea correlation for the Last Interglacial complex. *Earth and Planetary Science Letters* **171**, 123–37.

SÁNCHEZ-GOÑI, M. F., TURON, J.-L., EYNAUD, F., SHACKLETON, N. J. & CAYRE, O. 2000. Direct land/sea correlation of the Eemian, and its comparison with the Holocene: a high-resolution palynological record off the Iberian margin. *Geologie en Mijnbouw* **79**, 345–54.

SARJEANT, W. A. S. 1970. The genus *Spiniferites* Mantell, 1850 (Dinophyceae). *Grana* **10**, 74–8.

SEJRUP, H. P. & KNUDSEN, K. L. 1999. Geochronology and palaeoenvironment of marine Quaternary deposits in Denmark: new evidence from northern Jutland. *Geological Magazine* **136**, 561–78.

SEJRUP, H. P. & LARSEN, E. 1991. Eemian–Early Weichselian N–S temperature gradients; North Atlantic–NW Europe. *Quaternary International* **10–12**, 161–6.

SHACKLETON, N. J., SÁNCHEZ-GOÑI, M. F., PAILLER, D. & LANCELOT, Y. 2003. Marine Isotope Substage 5e and the Eemian Interglacial. *Global and Planetary Change* **36**, 151–5.

SJØRRING, S., NIELSEN, P. E., FREDERIKSEN, J., HEGNER, J., HYDE, G., JENSEN, J. B., MOGENSEN, A. & VORTISCH, W. 1982. Observationer fra Ristinge Klint, felt- og laboratorieundersøgelser. *Dansk Geologisk Forening, Årsskrift for 1981*, 135–49.

STOVER, L. E., BRINKHUIS, H., DAMASSA, S. P., DE VERTEUIL, L., HELBY, R. J., MONTEIL, E., PARTRIDGE, A. D., POWELL, A. J., RIDING, J. B., SMELROR, M. & WILLIAMS, G. L. 1996. Mesozoic–Tertiary dinoflagellates, acritarchs and prasinophytes. In *Palynology: Principles and Applications. Volume 2* (eds J. Jansonius & D. C. McGregor), pp. 641–750. Dallas, Texas: American Association of Stratigraphic Palynologists Foundation.

TAYLOR, F. J. R. 1980. On dinoflagellate evolution. *BioSystems* **13**, 65–108.

THRONDSEN, J. 1969. Flagellates of Norwegian coastal waters. *Nytt Magasin for Botanikk* **16**, 161–216.

TURNER, C. 2000. The Eemian interglacial in the North European plain and adjacent areas. *Geology en Mijnbouw* **79**, 217–31.

TURNER, C. 2002. Problems of the duration of the Eemian interglacial in Europe north of the Alps. *Quaternary Research* **58**, 45–8.

VAN LEEUWEN, R. J. W., BEETS, D. J., BOSCH, J. H. A., BURGER, A. W., CLEVERINGA, P., VAN HARTEN, D., HERNGREEN, G. F. W., KRUK, R. W., LANGEREIS, C. G., MEIJER, T., POUWER, R. & DE WOLF, H. 2000. Stratigraphy and integrated facies analysis of the Saalian and Eemian sediments in the Amsterdam-Terminal borehole, the Netherlands. *Geologie en Mijnbouw* **79**, 161–96.

WALL, D. 1967. Fossil microplankton in deep-sea cores from the Caribbean Sea. *Palaeontology* **10**, 95–123.

WALL, D. & DALE, B. 1966. "Living fossils" in western Atlantic plankton. *Nature* **211**, 1025–6.

WALL, D. & DALE, B. 1968. Modern dinoflagellate cysts and evolution of the Peridiniales. *Micropaleontology* **14**, 265–304.

WEAVER, A. J. & HUGHES, T. M. C. 1994. Rapid interglacial climate fluctuation driven by North Atlantic ocean circulation. *Nature* **367**, 447–50.

WILLIAMS, G. L., BRINKHUIS, H., PEARCE, M. A., FENSOME, R. A. & WEEGINK, J. W. 2004. Southern Ocean and global dinoflagellate cyst events compared: Index events for the Late Cretaceous–Neogene. In *Proceedings of the Ocean Drilling Program, Scientific Results, vol. 189* (eds N. F. Exon, J. P. Kennett & M. J. Malone), pp. 1–98. College Station, Texas.

ZAGWIJN, W. H. 1983. Sea-level changes in The Netherlands during the Eemian. *Geologie en Mijnbouw* **62**, 437–50.

ZAGWIJN, W. H. 1996. An analysis of Eemian climate in western and central Europe. *Quaternary Science Reviews* **15**, 451–69.

ZANS, V. 1936. Das leztinterglaziale Portlandia-Meers des Balticums. *Bulletin de la Commission géologique de Finlande* **115**, 231–50.

ZONNEVELD, K. A. F. 1997. New species of organic walled dinoflagellate cysts from modern sediments of the Arabian Sea (Indian Ocean). *Review of Palaeobotany and Palynology* **97**, 319–37.

Appendix 1. Systematic palaeontology

Division DINOFLAGELLATA (Bütschli, 1885) Fensome *et al*. 1993
Subdivision DINOKARYOTA Fensome *et al.* 1993
Class DINOPHYCEAE Pascher, 1914
Subclass PERIDINIPHYCIDAE Fensome *et al*. 1993
Order GONYAULACALES Taylor, 1980
Family GONYAULACACEAE Lindemann, 1928
Genus *Operculodinium* Wall, 1967 emend. Matsuoka, McMinn & Wrenn, 1997
Operculodinium centrocarpum (Deflandre & Cookson, 1955) Wall, 1967 var. *cezare* de Vernal, Goyette & Rodrigues, 1989 ex de Vernal, here
Figure 6k–o

1989 *Operculodinium centrocarpum* var. *cezare* de Vernal, Goyette & Rodrigues, p. 2462, pl. 1, figs 8–11.

Holotype. de Vernal, Goyette & Rodrigues, 1989, pl. 1, figs 8–9, UQP 200–6B, England Finder reference O44/0; conserved in the palynology collection of GEOTOP, Université du Québec à Montréal. Also figured in de Vernal *et al*. (2001, fig. 3.4 in lower panel).

Remarks. This variety was not validly published in de Vernal, Goyette & Rodrigues (1989) because the holotype was not designated at that time (Greuter *et al*. 2000; ICBN Art. 37.1). This requirement is satisfied here. *Operculodinium centrocarpum* var. *cezare* has short, densely-distributed, tapering processes. It was originally described from low-salinity late-glacial deposits of Québec (de Vernal, Goyette & Rodrigues, 1989) along with *Operculodinium centrocarpum* form B (de Vernal, Goyette & Rodrigues, 1989, pl. 1, fig. 5–7; also known as *Operculodinium centrocarpum* Arctic morphotype in de Vernal *et al*. 2001, fig. 3.3; Fig 6h–j) which has more sparsely distributed processes. These two morphotypes are grouped as *Operculodinium centrocarpum* var. *cezare sensu lato* during counting in the present study (Fig. 4, Table 1). *Operculodinium centrocarpum* var. *cezare* and *Operculodinium centrocarpum* form B both seem to characterize cold and Arctic environments today (de Vernal *et al*. 2001). However, their peak abundance in the lowest part of the marine sequence at Ristinge Klint clearly indicates an affinity for very low salinities, and implies that low salinity rather than low temperature is the major controlling factor in their distribution elsewhere.

Subfamily GONYAULACOIDEAE (Autonym)
Genus *Spiniferites* Mantell, 1850, emend. Sarjeant, 1970
Spiniferites ristingensis sp. nov.
Figure 8c–l

2005 *Spiniferites* sp. 1. Head *et al.,* fig. 8d–g.

Diagnosis. A species of *Spiniferites* having an ovoid central body, with or without a short apical protuberance, and bearing membranous gonal processes joined by low sutural crests. Some processes are distally expanded to form irregularly polygonal platforms. The central body wall is formed of two wall layers of similar thickness. The pedium is smooth, and the tegillum forms small, densely distributed blisters and hollow undulations over the surface. The processes and sutural crests are formed of the tegillum and are distinctly

bilayered. The surface of the processes and sutural crests appears granulate.

Types. Holotype: depth 57 cm, slide 1; England Finder reference P8/1. Fig. 8c–g. ROMP 57997. Paratype: depth 57 cm, slide 1; England Finder reference H49/2. Fig. 8h–l. ROMP 57997.

Description. A spiniferate cyst having an ovoid central body. A short apical protuberance up to 1.0 μm is sometimes present, as on the holotype (Fig. 8c–g). The central body wall is bilayered. The pedium is smooth, and the tegillum forms small, densely distributed blisters and hollow undulations over the surface, a feature clearly seen in transverse optical section (Fig. 8d). The blisters have a maximum diameter of about 1.8 μm. In plan view, the wall may appear granular, with dots (less than 0.3 μm wide and mostly spaced 1.0 μm or less apart) representing points of contact between pedium and tegillum. The pedium and tegillum are each less than 0.3 μm thick, and the wall is between 1.0 and 1.8 μm in total thickness. Processes are gonal and membranous. They are joined by sutural crests that are mostly low (less than 2 μm), but may be higher where processes are closely adjacent, especially along the cingulum. Processes are either truncated distally or expanded to form irregularly polygonal platforms, some of which typically extend outwards at right angles to the process stem. The apex may have one or more narrow, spine-like processes (Fig. 8f). The processes and sutural crests are formed of the tegillum and are distinctly bilayered, with a space of up to about 0.5 μm between layers caused by the undulating nature of the tegillum. The surface of the processes and sutural crests appears granulate. Claustra occasionally occur on the processes and sutural crests, and occur on the cingular processes of the holotype. The sutural crests indicate a typical gonyaulacoid tabulation, with a descending cingulum that is displaced about 2.5 times its width. The sulcal plates (especially the adcingular margin of 1P) are sometimes faintly discernible by subtle lineations in the wall ornament. The archeopyle is precingular, type P(3"), and a low (*c*. 1.0 μm) sutural crest occurs along the archeopyle margin (Fig. 8g). The operculum is monoplacate and free.

Dimensions. Holotype: central body length 42 μm; maximum process length 14 μm. Range: central body length 39(43.0)49 μm; maximum process length 11(12.9)17 μm. Fourteen specimens were measured.

Etymology. Named after the type locality.

Comparison. Spiniferites ristingensis sp. nov. is distinguished by its membranous processes and by the wall structure of the central body. *Spiniferites ludhamensis* Head, 1996*b*, from the upper Pliocene of eastern England, has a similar wall structure but hollow, non-membranous processes and hollow sutural crests. *Spiniferites delicatus* Reid, 1974, from modern sediments of the British Isles, has processes of similar shape but connected by high sutural crests, and a central body wall structure characterized by a pedium with radial fibres and a thin granular tegillum whose surface appears microgranular to microreticulate. *Spiniferites delicatus* also differs in having a reduced archeopyle.

Occurrence. Presently known only from the Eemian of the Baltic region; occurring persistently but in low numbers through zones RKDf 2 and 3 (reaching 3.7 % in RKDf 3) at Ristinge Klint, Denmark; in low numbers at Mommark, Denmark (M. J. Head, unpub. data); and sporadically and in low numbers at Lizce, Poland (as *Spiniferites* sp. 1 in Head *et al.* 2005). This species appears to tolerate reduced salinities judging from its early presence at the base of subzone RKDf 2a, although surface-water salinities nevertheless exceeded about 15 psu and bottom waters exceeded about 22 psu at this time (see Section 10.c).

Order PERIDINIALES Haeckel, 1894
Suborder PERIDINIINEAE (Autonym)
Family PROTOPERIDINIACEAE Balech, 1988
Subfamily PROTOPERIDINIOIDEAE Balech, 1988
Genus *Stelladinium* Bradford, 1975
Stelladinium sp. 1
Figures 11m–q, 12a, b, e

Description. Cyst is brown in colour, with a finely and faintly granulate surface. An apical, two lateral and two antapical horns are present, with none present on the cingulum. The tips of all horns are solid. The cingulum may be marked by a fold, the sulcus being weakly expressed or not expressed. A flagellar scar in the sulcal area is sometimes discernible. The archeopyle is intercalary, presumably 2a, offset to the right of the dorsoventral midline, and strongly asymmetrical in shape. The operculum is free. Accessory sutures appear to be developed in some specimens. Cyst length including horns 52(57.8)62 μm; cyst width including horns, 52(58.2)65 μm. Measurements are approximate as they include estimates based on incomplete specimens. Six specimens measured.

Remarks. Specimens differ from cysts of the extant *Protoperidinium stellatum* (Wall *in* Wall & Dale, 1968) Head *in* Rochon *et al*. 1999 (see Harland, 1982) in having shorter horns, and an archeopyle formed by loss of a single large intercalary plate in contrast to two attached intercalary plates in *P. stellatum*. Specimens differ from all known taxa of *Stelladinium* (see Fensome & Williams, 2004) in the combination of a relatively small overall size, short horns with solid tips, absence of cingular horns, and an archeopyle formed by the loss of a single intercalary plate.

Subfamily DIPLOPSALIOIDEAE Balech, 1988
or PROTOPERIDINIOIDEAE Balech, 1988
Genus *Echinidinium* Zonneveld, 1997 ex Head, Harland & Matthiessen, 2001

Remarks. The following two species are assigned only questionably to the genus *Echinidinium* because the nature of their archeopyle is uncertain or not observed. The only expression of tabulation (and hence dinoflagellate affinity) in *Echinidinium* is the archeopyle, which is theropylic and hence difficult to identify. It is therefore not certain that *Echinidinium*? sp. 1 and sp. 2 are even dinoflagellate cysts, although their small size, brown colour, acid-resistant walls and spinose ornament are all reminiscent of cysts belonging to the genus *Echinidinium*.

Echinidinium? sp. 1
Figure 10a–c

Description. Central body apparently subspherical originally, although specimens are now compressed and somewhat

crumpled. The wall is faintly to moderately granulate; processes are solid to apiculocavate, have a smooth surface, and taper to blunt or acuminate tips. Each specimen has a range of process sizes, so that some processes can be short and almost hairlike whereas others are long, wide-based (up to 2.5 μm) and apiculocavate. The range of process morphology on each specimen is itself variable. The central body wall and processes are light brown. The archeopyle is probably chasmic or theropylic, but crumpling of specimens prevents clear determination. Maximum diameter of central body, 32(39.3)47 μm; maximum process length, 3(4.3)7 μm. Twenty specimens were measured.

Echinidinium? sp. 2
Figure 10d, e

Description. Central body subspherical, with a smooth to faintly granulate surface. Processes are solid and hairlike, have blunt or acuminate tips, and are densely distributed so that process bases are about 1.0 to 1.5 μm apart. Processes on two specimens are mostly erect, and on one specimen are mostly recurved. Cysts are brown. An archeopyle was not observed. Maximum diameter of central body, 28–39 μm; maximum process length 2.0–2.5 μm. Four specimens were measured.